

Sphero-cylindrical Refraction with Spherical Lenses

Thesis

Presented in Partial Fulfillment of the Requirements for the Degree Master of Science in
the Graduate School of The Ohio State University

By

Joseph Christian Lehman

Graduate Program in Vision Science

The Ohio State University

2020

Thesis Committee

Thomas Raasch, OD PhD, Advisor

Bradley Dougherty, OD PhD

Heather Anderson, OD PhD

Copyrighted by
Joseph Christian Lehman
2020

Abstract

Purpose: To develop a meridional spherocylindrical subjective refraction method that does not require expensive equipment or extensive clinical training. To test the method empirically in normally-sighted subjects.

Methods: Participants were 35 young, normally sighted subjects with natural pupils and accommodation. Subjects viewed Gaussian-attenuated square wave gratings at four orientations (0° , 45° , 90° and 135°) with a 2.3 cycle/degree fundamental spatial frequency. The maximum plus spherical dioptric power for best subjective clarity was determined for each grating orientation, yielding the refractive correction needed in the four cardinal meridians. The spherocylindrical correction is represented by the one cycle sinusoid that best fits those data. Within- and between-session test-retest differences in M, J0, and J45 were calculated, as were astigmatic and total dioptric power differences. Goodness-of-fit metrics were derived from the differences in measured values within each orientation, and from the differences between the measured values and the best-fitting spherocylindrical power. Visual acuity was measured with each resulting spherocylindrical correction.

Results: In normally sighted subjects, median between-session test-retest differences for astigmatism are similar to published values for standard subjective refraction: ~ 0.13 D for both. Median differences for total dioptric power are larger than published values (0.26 D vs 0.20 D). The 95th percentile for astigmatic and total dioptric differences is larger by up to 40%, attributed to a greater number of outliers. LogMAR acuity is significantly correlated with the goodness-of-fit metrics.

Conclusions: In normally sighted subjects, this method results in median test-retest difference distributions that are similar to those found with standard subjective refraction. Mean and 95th percentile values for refractive components are larger than those for standard subjective refraction. Those differences are due to higher numbers of outliers, attributed to less effective control of overminussing some subjects. This problem of overminussing could be improved with modifications to the refraction procedure. The method could be adapted for use in settings in which full clinical resources and highly trained personnel are not available.

Dedication

To my brother Benjamin, for your determination and hard work in all you do; to my sister Rebecca, for your devotion and service to others; to my mother Suzanne, for your compassion and care for those you love; and to my father Jim, for your mentorship and guidance to me in our work, thank you.

To my future wife, Jenna Murray, for all your love and support, the joy and happiness you bring me, for the inspiration you give me every day, thank you.

Acknowledgments

I would like to thank Dr. Thomas Raasch for all of his guidance and support these past four years. I wouldn't have been able to complete this project without his expertise and assistance.

Vita

May 2012 Grove City High School
May 2016 B.S. Biology, The Ohio State University
May 2020 M.S. Vision Science, The Ohio State College of Optometry
May 2020 O.D. The Ohio State College of Optometry

Publications

Raasch T, Lehman J (2018). Meridional subjective refraction with spherical lenses and oriented targets. *Invest Ophthalmol Vis Sci* 58: E-Abstract 4758.
Lehman J Raasch T, (2018). Sphero-Cylindrical Refraction with Spherical Lenses. *American Academy of Optometry Poster Presentation*. 2018

Fields of Study

Major Field: Vision Science

Table of Contents

Abstract	ii
Dedication	iv
Acknowledgments.....	v
Vita.....	vi
List of Tables	viii
List of Figures	ix
Chapter 1. Introduction	1
Chapter 2: Methods.....	18
Chapter 3: Results	30
Chapter 4: Discussion	42
Bibliography	56

List of Tables

Table 1: Global Population of Blindness and Vision Impairment.....	12
Table 2: Statistical Values of Refractive Errors of the Subjective Sample	31
Table 3: Distribution of Standard Deviation of Test-Retest Differences	32
Table 4: Between-Session Test-Retest Repeatability of Subjective Refraction	45
Table 5: Between-and Within-Session Repeatability	49

List of Figures

Figure 2.1: Sequence of a Test Session	20
Figure 2.2: Gaussian-attenuated Square Wave Gratings	20
Figure 2.3: Example Dataset Plot	25
Figure 3.1: Distribution of Refractive Errors in Subjective Sample.....	31
Figure 3.2: Between-Session Test-Retest Differences in M, J ₀ , J ₄₅	33
Figure 3.3: Between-Session Test-Retest Differences in Astigmatism.....	34
Figure 3.4: Within-Session Test-Retest Differences in M, J ₀ , J ₄₅	35
Figure 3.5: Within-Session Test-Retest Differences in Astigmatism.....	35
Figure 3.6: Probability TRT Differences for astigmatism and total Dioptric Power.....	36
Figure 3.7: Datapoints at the Four Cardinal Meridians; Measurement SD	37
Figure 3.8: Goodness-of-fit Metrics	39
Figure 3.9: VA vs MSD; VA vs FSD	40
Figure 3.10: Distribution of Test Session Duration.....	40

Chapter 1. Introduction

Light travels at different speeds within different materials. The ratio of the speed that light travels in air to the speed that light travels in a material is its index of refraction. Light is refracted, or bent, when it passes between materials of different indexes of refraction. When light travels from material 1 to material 2, for example from air to water, the relationship between indices of refraction and the angle the light takes determines the amount the ray of light is bent. This relationship is described by Snell's law. These properties of refraction determine how light passes through and is focused in the eye.

The eye's refractive system, created by changes in curvature and index of refraction across the cornea and crystalline lens, focuses the light that passes through the eye. Physiologically, the clarity and health of these structures is an essential characteristic to promote a clear visual path. It is the relationship between the eye's refractive power and axial length that determines if this clear path for light creates a clear image. Light must be focused accurately onto the retina for a clear image to be formed.

Refractive error is the result of a disconnect in our eye's anatomical structure and its refractive capacity or power. When the axial length of the eye does not correlate to the focus point or focal plane, an out of focus image is formed on the retina. The amount the image is blurred and distorted depends on the amount of mismatch between the focus

plane and retina. Clinically, the refractive power and the vergence demand of the eye are not measured directly. Rather, the difference between the two is evaluated and measured. This difference describes the refractive error of the eye; a dioptric power that would result in an in-focus image on the retina.

Not all individuals fully develop emmetropia, where there is no mismatch in the structures of the eye. Individuals can stay hyperopic, where light is focused behind the retina, or myopic in which light is focused in front of the retina. When light is focused in front or behind the retina, a blur patch is cast on the retina with respect to this amount of refractive error. Even for the emmetropic eye, there is still a small blur circle due to diffraction and small amounts of higher order aberrations in the eye¹.

This optical error in the visual system has been studied substantially, focusing on development, treatment, and cause of refractive error. Initially, the vision of newborns is moderately hyperopic. At three months, the average infant has a refractive error $+2.16 \pm 1.30D$, meaning the focus of light is behind the retina. Extensive growth occurs during the third and ninth months resulting in a decrease of hyperopia and refractive error². Mutti et al showed that increase in axial length negatively correlated with the change in eye's refractive error. While the loss of refractive power due to changes in the lens and cornea increase the focal length, a decrease in hyperopic refractive error results from a greater increase in axial length. Consequently, a decrease in the variance and amount of refractive error in infants occurs².

The development of myopia is expected to occur during adolescence with an average age of onset of 10.4 years.³ Within the United States a third of individuals between 12 to 54 years old have myopia. It is estimated that by the year 2050 the prevalence of myopia worldwide will increase to five billion people, from just 2 billion in 2010.⁴ This is where light is focused in front of the retina. The development of myopia has been attributed to genetic inheritance and environmental factors, including time spent outdoors^{3, 5}. Studies on myopia control are currently establishing clinical standards for slowing the development of myopia. While in most circumstances the progression of myopia can only be decreased, this can be very impactful for individuals who would otherwise develop high amounts of nearsightedness. Currently clinically meaningful myopia control is defined as 30-50% decrease in progression⁶. With standard of care changing as new studies emerge currently three methods have evidence-based research supporting their use clinically. The treatment effect of multifocal and orthokeratology contact lenses, and atropine therapy all show promise⁷⁻⁹. While there is progress along the lines of myopia control, treatment is expensive and out of reach for even many in the United States.

Myopia's presentation and subsequent treatment by conventional means is straightforward. The diagnosis and prescribing for hyperopia in children is not as straightforward. A child with hyperopia can function with no negative symptoms with a moderate hyperopic refractive error.¹⁰ There are currently no standards for when to prescribe glasses for children with hyperopia; rather management is usually sign and symptom based. While these children can have uncorrected visual acuities with quick

reading at distance and near, hyperopia usually affects prolonged tasks. Often times poor performance in school or complaints of headaches and eyestrain will be the first clues that a child's visual system is causing problems.

Correcting refractive error reaches past clear vision. Amblyopia is the reduction in visual acuity attributed to neurologic deficits in the visual output of the eye not due to other pathology. There are three different causes for amblyopia, strabismic, deprivation, and refractive. Refractive amblyopia can be isometropic or anisometropic in nature. If left uncorrected, patients with amblyogenic refractive error risk factors are at risk for vision not developing correctly. There is a plastic period from infancy to 8 years during which if proper treatment is initiated permanent vision loss can be prevented. Identification of children at risk for amblyopia is difficult, as they can remain symptomless when the condition is unilateral. While one eye's visual system is not developing, the other is functioning normally. Treatment includes full correction of the refractive error, along with designated amounts of penalization of the good eye, forcing the underdeveloped visual system to be used.

The correction of refractive error is the backbone of the optometric profession. Blurred vision is almost always a component to a patient's presenting problem if not the chief complaint, most commonly due to uncorrected or under corrected refractive error. Refraction, a measurement of a patient's refractive error, can successfully be performed using many different methods clinically. Subjective refraction is typically performed as the sequential comparison of the clarity of images formed by two different lens powers¹. A typical procedure would start with the patient being blurred with excess plus power to

relax accommodation. Spherical power is determined by adding minus power in quarter diopter steps to optimize VA with the least amount of minus. Next, cylindrical power is determined using a Jackson cross cylinder lens and the flip-cross technique. The orientation of this lens is key to determining power and orientation of the cylindrical component. When the JCC principle meridians are in line with the subject's cylinder axis, the JCC can be used to determine cylinder power. If the principle meridians straddle the cylinder axis, the orientation of the cylinder axis is determined. Flipping the JCC exchanges the plus- and minus-powered axes, which allows the subject to compare the effect of change in clarity with cylinder power or axis changes. A patient's judgment of clarity and blur is used to arrive at an end point in lens power or orientation. Each successive presentation of lens powers is determined by the previous choice(s), with the final lens power expected to produce the best corrected visual acuity¹¹. At a point in each step, both lenses may seem equal in clarity, this is the ideal endpoint, termed bracketing. This type of procedure is considered the gold standard for the clinical measurement of refractive error. This procedure is utilized to prevent the over or under correction of a patient, and to ensure an accurate and efficient endpoint.

The first tools used to evaluate and eventually measure refractive error were termed optometers. The first optometer is considered to be Scheiner's disc, created in 1619¹ which used two pinholes and a distant light source to determine if ametropia is present. If the eye is ametropic, light is focused in front of or behind the retina, and two spots will be formed on the retina. In myopia, the top pinhole forms the bottom spot on the retina, and due to the inverted retinal image, will appear to be the top spot. If the top

pinhole is blocked, it appears to the patient that the top spot disappears. Of course, the opposite is true in hyperopia. The correct lens power will superimpose the two spots. If multiple meridians are tested, it is possible to measure astigmatic refractive errors.

In 1623 Benito Daza de Valdès created a simple optometer by using a strong plus lens and small mustard seeds. A plus powered lens is used in this apparatus to create an artificially myopic far point. A person's refractive error can be estimated by finding the position of the near object for best focus. In the years following, additional techniques were combined and improved upon. The name "optometer" was coined by Porterfield in 1759, and in 1801 Young used stenopaic slits instead of pinholes, and first described accommodation as the eye's mechanism to focus.¹² In 1876 Badal set the secondary focal point of an optometer to be at the spectacle plane, creating equally sized images with lens changes. The optometer was eventually combined with the phorometer, a device used to subjectively measure an individual's ocular alignment in the early 20th century.¹ The resulting device called a phoropter is the current tool used in most optometric clinics.

Improvements in refractive technology have often focused on automation. Auto- and objective refraction methods have been a frequently used tool in clinical settings. Automated phoroptors play an increasing role in clinical settings. While automated, many are still subjective instruments, i.e. the endpoints depend upon the subjective judgment of the patient. In contrast, objective refraction bypasses the judgment of the patient. Objective refraction serves an important role clinically. For example, when a patient is unable to give an accurate subjective response either due to development or a disability, their refractive state can still be examined with an objective refraction method.

Routinely, an objective measurement also serves as a starting point for the subjective measurement, creating a better starting point and decreasing test time. Retinoscopy, for example, has been the traditional form of objective refraction to provide a starting point for subjective refraction. Objective refraction can be more repeatable than subjective refraction performed by different clinicians on the same subject.¹³ Other objective methods now play the role of a starting point for refraction in many settings. Objective refraction is also often the method of choice for measuring refractive error in research, due largely to the finding that objective refraction can be more repeatable than subjective refraction. That is despite the widely held view that subjective refraction is the “gold standard” for refraction. That view is justified by the idea that subjective preference takes precedence over whatever an objective method would find.

Different technologies are used in objective refraction. For example, several autorefractors utilize the Scheiner’s disc principle in their design, including Topcon, Grand Seiko, and Nidek machines.¹ Other technologies, such as automated retinoscopy, or photo-refraction may also be used. In cases where a patient is not able to fully participate in a subjective refraction, an objective method may be used to find the final refractive error. Often, a patient’s subjective and objective results are both taken into account in the final corrective lens power prescribed. It is this combination of a patient’s visual preference, their visual demands, and balance of binocularity and accommodation that makes refraction an artform.

Studies that compare subjective and objective refraction have found different conclusions. For example, some find that subjective refraction is more repeatable, while others have found the opposite.^{13, 14} These different findings may result from different technologies and techniques being compared, different subject populations, and different types of data analyses. Current clinical opinion seems to be that subjective refraction remains the “gold standard” for refraction, but that various objective techniques have an increasingly important role due to improvements in accuracy, precision, and efficiency. However, it is likely that some form of subjective refraction will always be important, if only at a minimum to verify that the objective refractor found an acceptable result.

The impact of uncorrected refractive error has both individual and global consequences¹⁵⁻¹⁸. There are many who can function normally uncorrected, if the amount of error is low resulting in a smaller blur circle and functional VA. Children with small amounts of hyperopia are able to accommodate through low amounts of hyperopia, bringing the focal point towards the retina and decreasing the resulting blur circle. Even very small amounts of astigmatism and myopia, while causing a slight decrease in clarity, may not significantly affect a person’s everyday function. Commonly the relationship of refractive error to visual acuity that is expected is a quarter step of myopia will result in a one line decrease in visual acuity¹⁹. At -1.00 to -1.50 diopters of uncorrected refractive error, visual acuity will reach approximately 20/40 to 20/60. A VA >20/60 qualifies as moderate to severe visual impairment, having a significant effect on a person’s utility or quality of life. Similarly, if vision in an individual’s better eye is worse than 20/400, they

are considered blind. These terms are based on ICD-10 coding criteria, and under the assumption that these are an individual's best corrected acuities.

The effect of uncorrected refractive error on quality of life for adults can come from its effect on job performance, on limiting function and interaction with life.

Refractive error, if left uncorrected, should be treated as equal to other forms of vision loss such as glaucoma and macular degeneration. Multiple studies have shown the effect uncorrected refractive error has on an individual, and there are many different metrics used to express these negative consequences.

Utility is a measure used to quantify an individual's quality of life, reduced to a single number ranging from 0 (death) to 1 (perfect health). In this way, the impact of separate diseases and conditions can be directly compared and correctly prioritized. A cross-sectional study of uncorrected refractive error investigated the impact it has on an individual's utility compared it to previously published data on other ocular diseases such as glaucoma and AMD. The decrease in VA due to uncorrected refractive error resulted in a similar decrease in utility as these visually devastating diseases.¹⁷ Individuals with ocular pathology did have a slightly lower utility, due to both near and distance vision being compromised. Separately, reduced near or distance acuity due to uncorrected refractive error affect an individual's utility equally. When both near and distance vision are affected, as in an eye affected by an underlying disease, quality of life is decreased greater. Typically, with uncorrected refractive error, either near or distance vision will be affected, as described in the terms nearsighted and farsighted. The impact of reduced

distance VA and its influence on utility has been studied extensively; however, the effect of decreased near acuity, specifically presbyopia has not.

Another unique epidemiology measure is disability-adjusted life years (DALY). This metric takes into account the years lost due to premature death, and the years lived with the disability or disease. In contrast to measurement of utility and the impact of an individual's quality of life, DALY can be used to compare different pathologies on a larger scale. Notably, DALY statistics have been used to compare causes for disability in over 118 countries, including uncorrected refractive error.²⁰ It was found that of all other eye conditions and pathology, uncorrected refractive error has the greatest burden based on disability, and is comparable in impact to diseases such as syphilis and alcohol abuse disorders. One large difference in the effect on quality of life is said to be due to the nature of a disease, and the fear of possible progression, whereas refractive error can remain stable after adolescence¹⁷.

As seen in other socioeconomic areas, disparities are found comparing men and women in areas where uncorrected refractive error is high. In a Sri Lankan study uncorrected refractive error was found to be codependent on both age and sex. While there was an equal number of males and females with uncorrected refractive error, elderly females and young men were more likely to have uncorrected refractive error.¹⁵ Unfortunately, children are affected by uncorrected refractive error more significantly than adults. For children, uncorrected refractive error can greatly affect their education and development. Using a low vision quality of life questionnaire, the quality of life for children with vision impairment was reduced by 35.6%.^{21, 22} As mentioned above, during

the ages of 5-12 children with certain refractive error are at risk for amblyopia. This would limit the visual ability possible throughout life even if corrected in the future.

Due to the significant number of individuals who suffer from uncorrected refractive error, there is a negative global economic impact. Uncorrected refractive error not only affects an individual's quality of life, but also limits their contribution to society. The cost of provided aid was taken into account in estimating the economic impact of uncorrected refractive error. To properly calculate global effect, differences in cost of living and difference in pricing in different countries were corrected for based on purchasing power parity (PPP). The yearly potential lost productivity was estimated at 202 to 268 billion dollars gross domestic product loss (GDP) PPP adjusted.^{23, 24} While the predicted loss of production due to uncorrected refractive error is devastating; the estimated cost of providing both an exam and glasses to those in need was 26 billion dollars.²⁵ This is approximately a factor less than the predicted financial burden uncorrected refractive error can cause, and a sign that measures need to be taken to reduce the total number of individuals affected.

In 1999 the world health organization (WHO) and the International Agency for the Prevention of Blindness (IAPB) established the VISION 2020 Right to Sight initiative. The initiative's focus was to eliminate the increasing number of preventable vision impairment and blindness in the world. Blindness was defined as vision worse than 20/400 in the better eye, with targeted diseases including cataracts, trachoma, onchocerciasis, glaucoma, and diabetic retinopathy. The IAPB covers seven regions of the world: Africa, Eastern Mediterranean, Europe, North America, South America,

Southeast Asia, and Western Pacific. Common issues facing each region included lack or maldistribution of manpower and trained eyecare professionals and lack of facilities.¹⁸

Table 1. Global population with blindness and vision impairment. Numbers in millions. (URE) Uncorrected Refractive Error. (VI) Vision Impairment

Year	Blindness	Blindness due to URE	VI	VI due to URE
1990	31.8	6.4	172.0	87.8
2010	32.4	6.8	191.0	101.23
2015	36.0	7.4	216.6	116.3

Uncorrected refractive error is the second leading cause of blindness in the world, and the number one cause of vision impairment in the world. Initial estimates before Vision 2020 and follow up studies by the IAPB are found in Table 1. The most current numbers from Flaxman et al. estimate the number of individuals with VI to be 216.6 million with 116.3 million of those cause by uncorrected refractive error. Additionally, 36.0 million people who are blind with 7.4 million of those caused by uncorrected refractive error.²⁶

While the prevalence of blindness and moderate to severe vision impairment have decreased over the last 20 years, the gross number of people affected continues to increase as seen in Table 1. As the world population continues to increase in number and age, it is expected that the number of individuals with uncorrected refractive error will increase. This indicates that further intervention and action is needed, to fully address an issue caused by lack of action.

Notably at the beginning of VISION 2020, uncorrected refractive error was not included when establishing the goals for decreasing VI and blindness. The surveys taken for estimating the number of people with VI or blindness used current ICD-10 definitions, which are determined by best corrected VA.²⁷ In comparison to the other pathological causes that take additional time for treatment, uncorrected refractive error is an immediately correctable problem. The original number of blind people in 1999 was estimated at over 45 million²⁸.

It is evident that there is a great unmet need for correction of refractive error, and lack of access to refraction contributes significantly to this unmet need. Whether refraction is performed subjectively or objectively, there are significant resources that are required. Extensive training to perform and interpret subjective refraction and expensive equipment such as an autorefractor or phoropter are needed for almost all clinically standardized refraction techniques. In areas without the resources individuals with uncorrected refractive error are subject to a decrease in quality of life. In addition, there are significant economic consequences in areas of epidemic uncorrected refractive error.

Analysis of spherocylindrical measurements is not a straightforward mathematical process. This is due to the nature of spherocylindrical notation. The quantities of sphere power, cylinder power, and cylinder axis can be represented as a form of polar notation, where sphere specifies the spherical refractive error, and astigmatic refractive error is represented by the polar notation cylinder power (magnitude), and cylinder axis (orientation). Sphero-cylindrical powers, when represented in this way, do not allow simple statistical analysis techniques, and if analyzed incorrectly will yield incorrect

results²⁹. Due to the interactions between sphere, cylinder and axis, spherocylindrical powers must be transformed to a different coordinate system before analysis. A coordinate system in which there are three mutually-orthogonal axes can be used to specify spherocylindrical powers and will allow for simple statistical analysis.

Spherical equivalent, M, is one of the three axes in that system. It is defined as the sphere power plus half the cylinder power. Spherical equivalents are commonly used in the clinical setting to compare changes in spherocylindrical power crosses. Typically, astigmatism is represented by a cylinder power and axis. With vector analysis, the astigmatic power is represented along two orthogonal axes, referred to as “J₀” and “J₄₅”. Because sphere, cylinder, and axis values are not independent of each other, manipulation and analysis of the values cannot happen independently³⁰. For example, a cylindrical lens such as (0.00 – 1.00 x 180) has a spherical equivalent value (-0.50D). In spherocylindrical notation, this non-zero spherical power is not accounted for in statistical analysis. In response to this issue, spherical equivalents have been used in statistical analysis. This however neglects the orientation of any cylinder power in the original spherocylindrical lens. For example, two lenses both with a spherical equivalent of -1.00D, potentially correct different axis orientations. When a spherocylindrical power is expressed as spherical equivalent, J₀, and J₄₅, arithmetic and statistical operations can be performed appropriately, without issues arriving from the non-orthogonality of those values.

The traditional notation of lens power can be expressed as vectors in this three-dimensional space, and are independent of each other, and represent the same spherocylindrical power lens. Vector notation of lens power represents the three-dimensional (X,Y,Z) Cartesian coordinates. The vector notation separates spherical power and cylindrical power, as well as separating cylindrical power by orientation. The first vector M (or spherical equivalent) is calculated as sphere power plus one half the cylinder power. The astigmatic power is defined by J0 and J45. J₀ is ½ the difference in power between the 0 and 90 degree meridians. J₄₅ is ½ the difference in power between the 45 and 135 degree meridians. With this notation, individual values can be statistically analyzed independently of each other. It often makes sense to represent spherocylindrical powers using this approach, including when communicating findings to the larger community, including non-optometric personnel.

This vector notation creates a more intuitive representation of refractive error in that there is no requirement for understanding spherocylindrical power cross notation (e.g. Sph ⊂ Cyl x Axis). While most individuals can understand the description of spherical lens power and the function of convex and concave lenses, cylindrical lens power and orientation is not so easily comprehended. If vector notation could be utilized in clinical refraction, the limiting factor of spherocylindrical power relationships would be avoided¹¹. This project describes an approach to clinical subjective refraction in which spherical equivalent, J0 and J45 are measured more directly than is done with standard subjective refraction. It can be performed with less specialized equipment, and

likely can be done competently by personnel who are not as fully trained as is otherwise necessary.

Revert et al¹¹ proposed a similar alternative subjective refraction technique involving vector notation to determine final spherocylindrical lens power. JCC lenses were utilized to isolate meridians. Tumbling E Snellen charts were used at the typical (0, 90, 180, 270 degree) rotations and an alternative chart with (45, 135, 225, 315 degree) rotations. This study showed that alternative subjective refraction techniques using vector refraction were comparable in time and repeatability to current subjective refraction. Revert et al expressed that while the statistical evidence for vector refraction was comparable to standard subjective refraction methods, there needs to be further study on the subjective acceptance of the produced correction.

In normal eyes, with low levels of aberration, subjective refraction may be only slightly affected by higher order aberrations. In eyes with higher levels of aberration, however, those effects are expected to be more pronounced. One type of effect is that higher order aberrations (HOAs) can shift the optimum sphero-cylindrical correction from where it would be without those HOAs. Another effect is that subjective refraction in highly aberrated eyes is more variable and it is more difficult to find a confident endpoint. The effect of different types of aberrations on the retinal image are varied. Letter targets are complex in the sense that they contain multiple spatial frequencies at multiple orientations. The effects of aberrations on letter images can be described as “smearing” or asymmetrical blurring, doubling or ghosting, or shape distortions. When faced with the subjective judgment of “What’s better, 1 or 2?”, those varied effects can

produce two quite different retinal images for choices “1” and “2”, but with no obvious answer to the question of which one is better. Oriented line targets, however, are simpler since they consist of a single orientation and a limited number of spatial frequencies. The primary effect of blur from either sphero-cylindrical blur or from aberrations is to reduce the contrast of those gratings. The targets used in this study are square-wave gratings, so multiple spatial frequencies are present, but the main effect of blur is still contrast reduction. That suggests, especially for highly-aberrated eyes, that this type of subjective task could be less variable and easier to perform because the judgment of which is better is simply to identify the higher contrast, rather than choosing between differently smeared, ghosted, and blurred letters.

The purpose of this study is to evaluate an alternative subjective refraction technique. There is potential value in a method that would allow for the use of inexpensive tools and a less complex refraction that could be taught quickly to an inexperienced clinician. The method tested will use spherical lenses and linearly oriented targets to isolate individual meridians. Repeatability of the study was evaluated by comparing test-retest difference with and between refraction sessions. Computer adapted visual acuity measurements were taken and used with goodness of fit metrics of refraction precision and consistency to evaluate the accuracy of the refraction.

Chapter 2: Methods

A. Inclusion/Exclusion Criteria, Subject Population, and Sample Size

1. Inclusion/Exclusion Criteria and Subject Population

To be eligible, potential participants had to be age 18 years or older, have corrected visual acuity of 20/25 or better OD and OS, and have no history of significant eye disease or ocular injury. There was no restriction on refractive error or type of correction worn. Subjects were recruited primarily from the student population at The Ohio State University College of Optometry. Subjects were asked to have the same optical correction available for test and retest sessions. At the first visit, eligibility was confirmed by verifying age and reported ocular history. Eligibility based on visual acuity was verified as part of the testing. Both eyes of subjects were tested. The study was reviewed and approved by the OSU Biomedical Institutional Review Board.

2. Sample Size

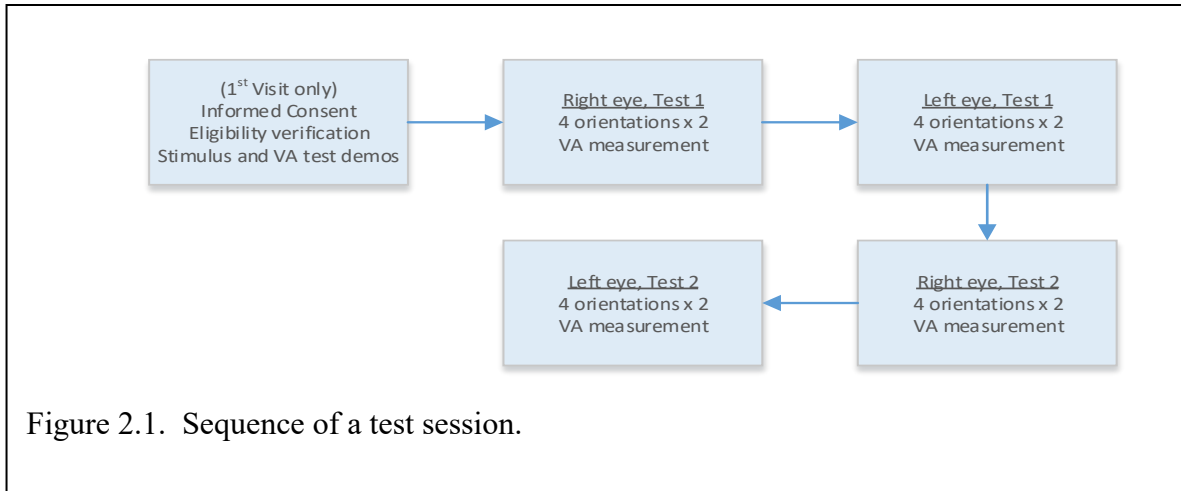
A sample size estimate was generated using two statistical methods: from a Chi-squared test for equality of variance, and with a “bootstrap” method. The test-retest variance in total dioptric power in standard subjective refraction was estimated from a large study in which a standard refraction protocol had been implemented in a reasonably large number of normally-sighted myopes³⁰. From that study, the estimated standard deviation of test-retest differences in total dioptric power is 0.316 D, or a variance of 0.10 D². Calculated

sample size was powered to detect a 2x greater ratio of variances, or a ratio of standard deviations of $\sqrt{2}$ x between meridional refraction and standard refraction, with $p = 0.05$ and power = 0.80. This calculation yields a needed sample size of 26 subjects. The bootstrap method used a randomly generated sequence ($n=10,000$) of values, with standard deviation $\sqrt{2}$ x the standard deviation of the standard refraction method, with 4 to 60 subjects at each of those 10,000 iterations. The 80th percentile p-value (for 80% power) drops below 0.05 at 26 subjects. To account for possible dropouts, losses to follow-up, etc., and to increase power, this was increased to 35 subjects. If all 35 subjects successfully completed all tests, the study would be powered to detect a standard deviation ratio of 1.34x.

B. Testing Procedures

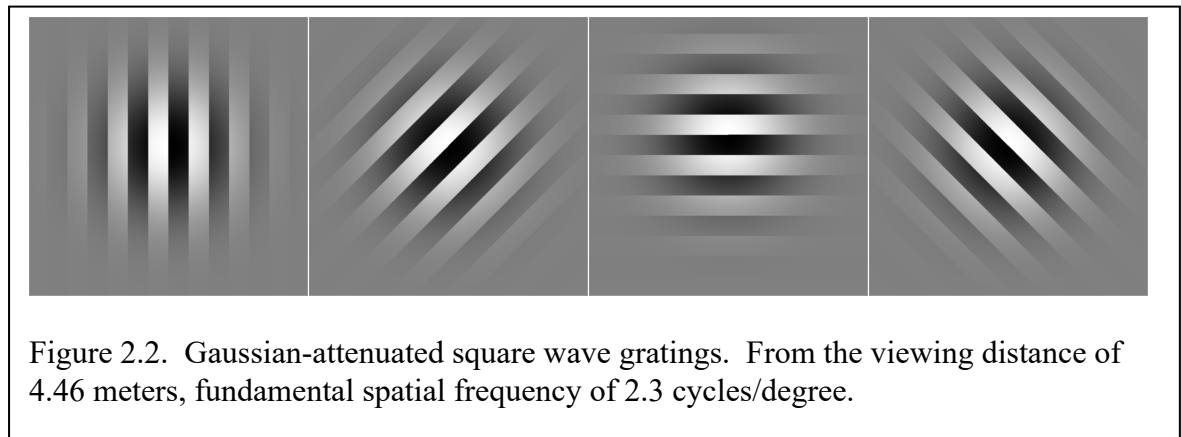
1. Test Components and Sequence

The sequence of a full test session is illustrated in Figure 2.1. Both eyes were tested, and visual acuity was measured with the results of each measurement. The details of these tests are described below. This sequence of testing was repeated at the second visit, which followed the first visit by from 1 to 2 weeks. All stimulus presentations and experimental control and sequencing was computer-controlled, using MATLAB (The Mathworks, Natick MA). Duration of testing was measured and recorded by computer. Data were recorded as digital Matlab (*.mat) files, with hand-recorded hardcopy backup.



2. Visual Targets

Visual targets were displayed on an LCD computer screen (1280 x 1024 pixels, 340 x 272 mm, mean luminance 100 cd/m²). The screen was viewed from a distance of 4.46 meters, yielding an angular pixel size of 0.205 minarc/pixel. Stimuli were Gaussian-attenuated square wave gratings with a fundamental spatial frequency of $f = 2.3$ cycles/degree. Since this was a square wave grating, higher frequency components were: $3f$, $5f$, $7f$, etc., at contrasts relative to that of the fundamental of $1/3$, $1/5$, $1/7$, etc., respectively. Those higher frequencies give the gratings the sharp edges. Without those



higher frequencies, the grating would be a simpler sinusoidal grating. The Gaussian envelope attenuated grating contrast to 50% at a radius of 1.4 cycles of the grating, meaning that the contrast decreased from 100% in the center to near zero at the image edge. Figure 2.2 illustrates these gratings. Square wave gratings, rather than a single frequency sinusoid, were used, based on the hypothesis that the higher frequency components, and hence the sharp edges, would enable subjects to detect smaller changes in focus clarity. The Gaussian envelope attenuation of grating contrast was used to minimize extraneous edges at orientations other than that of the displayed grating.

3. Meridional Subjective Refraction

Four orientations of the grating were used: 0° , 45° , 90° , 135° . A minimum of 3 meridians were needed to produce a spherocylindrical prescription. One grating was shown at a time, with sequence either randomized, or in sequence from 0° through 135° . At each orientation, gratings were viewed through spherical lenses in a standard manual phoropter. Starting at a lens power to produce blur with excess plus power, power was decreased in 0.25 D steps to attain maximum clarity. The endpoint was the maximum plus/minimum minus dioptric power that maintained maximum clarity of the target, based on the subjective response of the subject. No dilating or cycloplegic eyedrops were used.

The sharpness of focus of grating edges is determined by the dioptric power in the meridian orthogonal to grating orientation. For example, for the vertical grating, the power in the horizontal meridian determines the quality of focus of the vertical edges. Likewise, the power in the vertical meridian determines the focus of the horizontal

grating. The grating oriented (from the subject's perspective) 45° clockwise from vertical yields the correction for the 45° meridian. Referring to the four images in Figure 2.2, as viewed by the subject, the relevant meridians for the images from left to right are 0° , 45° , 90° , and 135° . Orientation specification is consistent with the clinical convention of 0° being on the patient's left (or examiner's right), with the positive rotation angle being counter-clockwise (from the examiner's perspective). The dioptric power at those four orientations allows calculation of the correcting spherocylindrical power, as described below in Section C.

4. Visual Acuity Measurement

Following each set of eight power determinations, visual acuity was measured with the sphero-cylindrical result, with sphere and cylinder powers rounded to the nearest 0.25 D. That result was dialed into the phoropter, and optotypes were displayed on the same computer screen at the same distance. Visual acuity was measured using a computer-controlled, adaptive staircase method, as described in detail in Andrews³¹. That visual acuity measurement algorithm is briefly described below.

Optotypes were in Sloan font, as black letters on a white background, using the 10 uppercase letters used in Early Treatment Diabetic Retinopathy Study (ETDRS) charts:

C D H K N O R S V Z

Available letter sizes were from 50 minarc (20/200) to 1.25 minarc (20/5), in 0.05 log unit steps. On screen, the largest and smallest letters were 65 mm (~ 250 pixels) and 1.62 mm (~ 6.25 pixels) on a side. Rendering the smallest available letters with just 6.25 pixel

height produced degradation of detail. However, the smallest threshold letter sizes were expected to be approximately twice this smallest available size.

Letters were shown one at a time without surrounding letters or crowding bars. The appearance of each letter was accompanied by a brief, computer-generated beep. Each letter was displayed until the subject responded with a button press on the keyboard. Alternatively, the subject could speak the letter, which was then typed by the examiner. Any response other than one of those 10 letters was not accepted by the computer, and was accompanied by a low-tone beep, signaling the subject to make a different selection.

Letter size started at a size sufficiently large to assure a correct response. The adaptive staircase used a modified “ZEST” algorithm for determination of subsequent letter sizes³¹⁻³³. A probability density function (PDF) tracked the relative probability of threshold size being at any particular location after each letter presentation and response, across a wide size range. After each letter presentation and response, the PDF generally becomes narrower (i.e. more sharply peaked) and shifts to smaller sizes (after a correct response) or to larger sizes (following an incorrect response). The general strategy behind this adaptive method is to concentrate most presentations at letter sizes near threshold. Each of the 10 letters was shown five times, in random sequence, so each measurement consisted of 50 letter presentations. In keeping with a ZEST procedure, the final visual acuity was taken as the location of the “center of gravity” of the PDF along the letter size axis.

C. Data Processing and Analysis Methods

1. Determination of Sphero-cylindrical Correction from Meridional Data

Figure 2.3 illustrates the calculation of refractive results, using an example set of data.

The data points appear on the horizontal axis at 0° , 45° , 90° , and 135° . The vertical axis is dioptric power. The bold red curve is the best fit, one-cycle sinusoid that minimizes the sum of squared differences between the measured points and the curve and represents the sphero-cylindrical correction. In minus-cylinder form, the sphere power is the power at the peak of this curve, the cylinder power is the peak-valley difference in power, and the cylinder axis is the horizontal location of the peak. In this particular case, those values are: Sphere = -0.58 D, Cylinder = -1.35 D, Axis = 146° .

In dioptric vector format, the spherical equivalent, or M , is the mean height of this curve, J_0 is the one-cycle cosine component, and J_{45} is the one-cycle sine component. In this case, those three values are shown by the horizontal dashed line (M), and the one-cycle dashed curves in cosine (J_0) and sine (J_{45}) phase. The cylindrical magnitude, or J , is the Pythagorean sum of J_0 and J_{45} , i.e. $J = \sqrt{J_0^2 + J_{45}^2}$.

When the empirical measurements are made at these four specific meridians, these three components are easily calculated: M is the mean value of the measurements, J_0 is half the difference between the 0° and 90° values, and J_{45} is half the difference between the 45° and 135° values. Formally, those calculations are:

$$M = \frac{1}{4} \sum_{i=1}^4 p_i, \quad J_0 = \frac{p_1 - p_3}{2}, \quad J_{45} = \frac{p_2 - p_4}{2}, \quad J = \sqrt{J_0^2 + J_{45}^2} \quad (1)$$

where p_{1-4} is the power at 0° , 45° , 90° , and 135° , respectively.

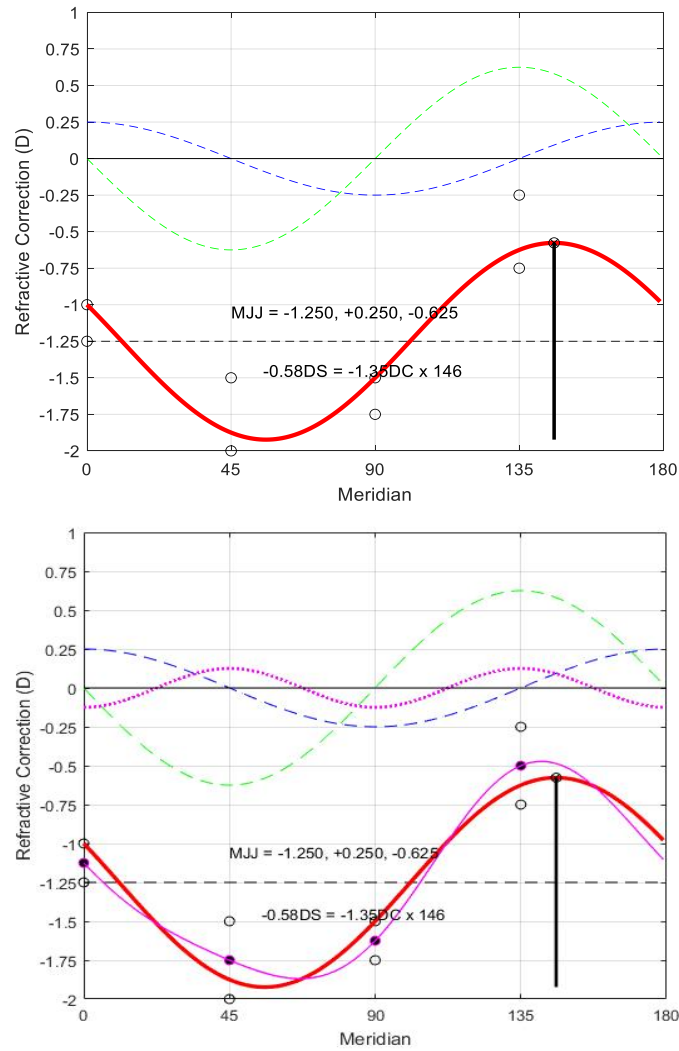


Figure 2.3. Example dataset.

Top: Two datapoints at each of the four cardinal meridians. Bold red curve represents the best-fitting sphero-cylindrical power. The dashed curves represent M (horizontal at -1.25 D), J_0 (blue), and J_{45} (green). The sum of those three is the bold red curve.

Bottom: The solid black datapoints are the mean of the measurements at each orientation. The added 2-cycle curve (dotted magenta) represents the mis-fit of the one-cycle curve to the data. The sum of all components (i.e. M , J_0 , J_{45} , and 2-cycle curve) is the solid magenta curve, fitting the data exactly.

Given this data set, those values yield:

$$\begin{aligned}
 M &= \frac{-1.125 - 1.75 - 1.625 - 0.5}{4} = -1.25D, & J_o &= \frac{-1.125 + 1.625}{2} = 0.25D, \\
 J_{45} &= \frac{-1.75 + 0.5}{2} = -0.625D, & J &= \sqrt{0.25^2 + (-0.625)^2} = 0.673D
 \end{aligned}
 \tag{2}$$

2. Determination of Sphero-cylindrical Correction with a Discrete Fourier Transform

If some number other than four orientations is tested, a more general method for finding M , J_0 and J_{45} is needed. One possible approach is to use a curve-fitting algorithm.

Another effective approach is the discrete Fourier transform. A minimum of three orientations is required, and they must be uniformly distributed across the 180 degrees of orientation: in this case 0° , 45° , 90° , and 135° . If just three orientations were tested, those would be 0° , 60° , and 120° . This three-meridian refraction has been used in photorefractive protocols³⁴, although the data in these previous reports of photorefractive were not analyzed using a discrete Fourier transform approach.

A discrete Fourier transform yields, for n orientations, a set of n complex numbers. Depending upon the normalization method of the particular discrete Fourier transform algorithm, these numbers may have to be normalized, i.e. divided by n . This is the case if the Matlab “fft.m” function is used. The first number is always real-valued and is generally called the *DC* value. In this context, this is the mean, or M value, in diopters. The 2nd and 4th complex numbers in the series are redundant, i.e. they are complex conjugates of each other. The 4th number (multiplied by 2) is the one-cycle component. The real part of this complex number is the cosine, or J_0 , component, and the

imaginary part is the sine, or J_{45} , component. In this example, M , J_0 , and J_{45} are: -1.25 D, +0.25 D, and -0.625 D (consistent with Equation 2 above). The J_0 component is the one-cycle cosine wave with amplitude +0.25 D, and the J_{45} component is the one-cycle sine wave with -0.625 D amplitude. Given this example data set, a discrete Fourier transform yields this complex result:

$$\begin{array}{l} \mathbf{-1.25} \\ 0.125 + 0.3125i \\ -0.125 + 0i \\ \mathbf{0.125 - 0.3125i} \end{array}$$

The first number is the value of M (-1.25 D). The real part of the last number x 2 is J_0 , (+0.25 D), and the imaginary part x 2 is J_{45} (-0.625 D).

If four or more orientations are tested, four or more complex numbers result from the discrete Fourier transform. The additional complex numbers (other than the first, second, and last numbers) represent higher-frequency components, and indicate how well the one-cycle sinusoid (i.e. the spherocylindrical correction), fits the measured data points. In this example, with four complex numbers, the third number is the 2-cycle component, and in Figure 2.3 is the dotted 2-cycle sinusoid. It represents the magnitude of misfit of the one-cycle curve to the measured data. In this example, it has a magnitude of -0.125 D. Note that $M + J_0 + J_{45}$ equals the spherocylindrical correction. The sum of all components (i.e. adding to that sum the 2-cycle component) perfectly fits the data at the four orientations and is shown as the solid magenta curve. This discrete Fourier transform method of finding spherocylindrical components from multiple meridional powers is similar to a method described previously³⁵. It has elements of a Zernike approach, in the sense that the azimuthal variation in power is decomposed into harmonic

frequencies. It differs from a Zernike approach in that it does not indicate variation in power with radial distance from the aperture center.

3. Reliability, Validity, Goodness-of-Fit, and Efficiency

A primary data analysis in this study is the evaluation of reliability, using a test-retest repeatability analysis method. Test-retest analyses include those within a session, and between sessions. The distribution of test-retest differences is compared to the distribution of test-retest differences in standard refraction, derived from the published literature. In addition, visual acuity results are used as a test of the accuracy, or validity, of the method. That is, a refractive error measurement that results in a better visual acuity is an indication that that measurement is more accurate. As described above, visual acuity was measured with the results of each refractive endpoint using an adaptive staircase method.

Goodness-of-fit was evaluated in two ways; by how well the sinusoid matched the measured data points, and by the discrepancies between the two measured values at each orientation. First, the fit of the raw data to the best-fitting sphero-cylindrical correction is used as an indication of how completely that correction compensates the refractive error. The example shown in Fig. 2.3 shows that at each of the measured orientations, the best fitting sinusoid deviates from the mean of the measured values at each orientation by either +0.125 D or -0.125 D. Those differences are seen in the 2-cycle sinusoid, which has an amplitude of 0.125 D. This goodness-of-fit value is referred to as the fit standard deviation. It is hypothesized that the fit standard deviation is related to the level of higher-order aberration of that eye. Mismatch between the produced one-cycle sinusoid

and average meridian refraction endpoints is relatively small for normally sighted individuals. As the amount of higher order aberrations increase, the fit standard deviation is expected to increase.

The other metric used to characterize goodness-of-fit is derived from the differences between the two measured values at each orientation. In Fig. 2.3, those four differences are 0.25 D, 0.50 D, 0.25 D, and 0.50 D. That statistic is termed the MsmtSD (for “measurement standard deviation”), and is calculated as the square root of the sum of the squared differences at each orientation, divided by the number of orientations, or:

$$MsmtSD = \sqrt{\frac{\sum_{i=1}^4 (p_{i,2} - p_{i,1})^2}{4}}, \text{ where } i \text{ represents the four orientations, and } p_{i,1} \text{ and } p_{i,2}$$

represent the two measurements at each orientation. For the data shown in Fig. 2.3, this value is 0.395 D. The possible significance of this statistic is that it reflects the consistency of responses of the subject. A number of factors may contribute to that level of consistency, one of them being the aberrations of the eye; the higher the level of aberration, the more blurred and irregular the retinal image, and the more likely the subject will be inconsistent in their responses.

Finally, the efficiency of the method was evaluated by analyzing the duration of the testing sessions. The overall duration of each testing session was recorded by the software controlling the sequence of tests.

Chapter 3: Results

All subjects were age 18 years or older, and a majority were current students or staff at The Ohio State University College of Optometry. All subject visits were conducted between June 23 and November 11, 2017. The full cohort of 35 subjects was recruited, and no subjects were found to be ineligible following recruitment. The median interval between the first and second visits was 10 days, with most second visits occurring between 7 and 14 days. The inter-visit interval for three of the 35 subjects fell outside the prescribed two week maximum interval. It was judged, however, that this would not introduce systematic bias into the results, so those results were retained in the analysis.

For each refraction of each eye of each subject, the refractive correction was calculated according to the procedures described in Chapter 2. Methods, Section C. Each refraction consisted of 8 power determinations: 2 determinations at each of the major meridians (0, 45, 90, 135 degrees). Visual acuity was measured with the results of each refraction using methods described in Chapter 2. Methods, Section B.³¹

The statistical distributions of the refractive errors of the subject sample are listed in Table 3.1, and shown in Figure 3.1. All values are in diopters. These values yield a mean refractive correction, in minus-cylinder form, of:

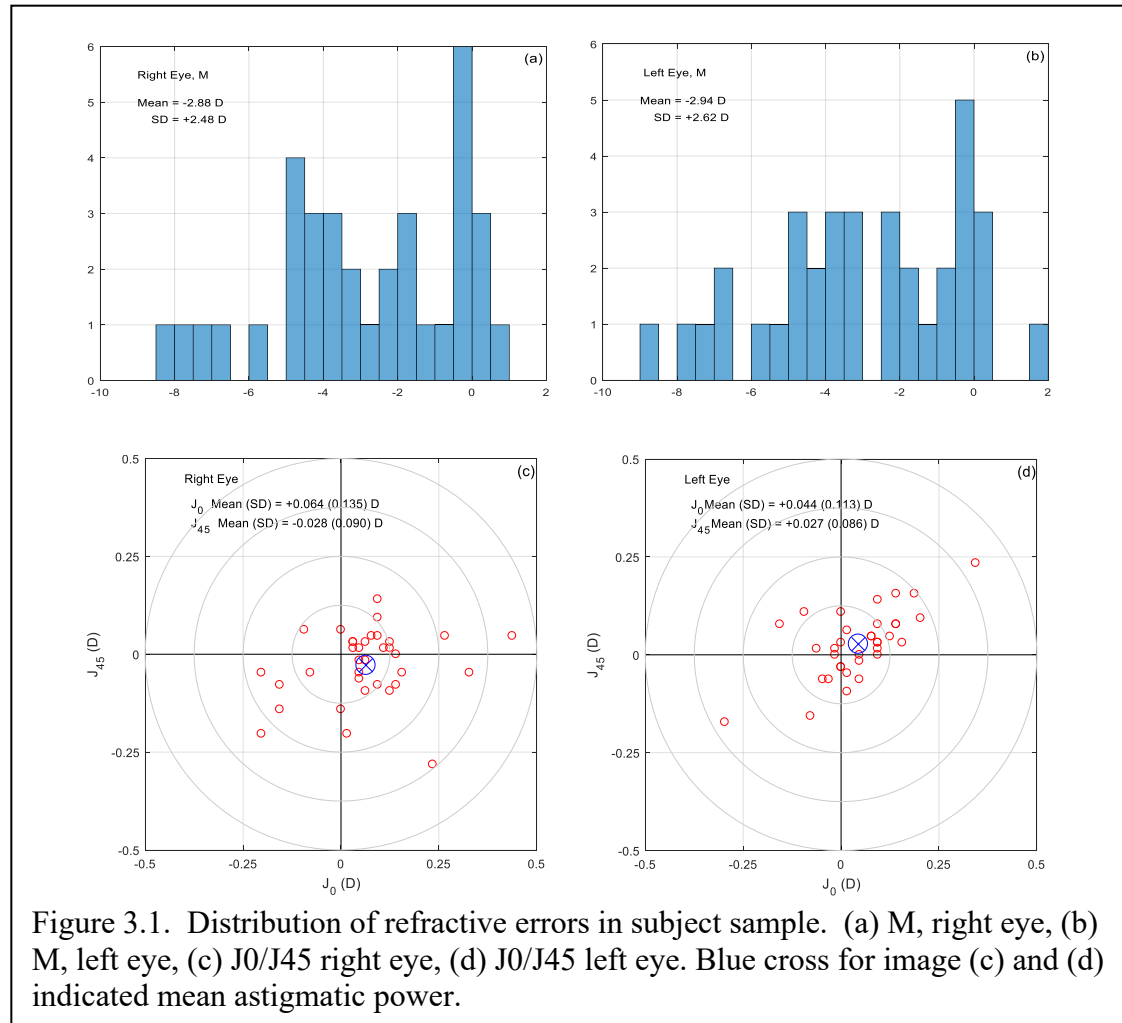
OD: -2.81 - 0.14 x 168

OS: -2.89 - 0.10 x 016

Not unexpectedly, this subject sample was predominantly myopic, with small amounts of with-the-rule astigmatism with mirror-image symmetry.

Table 2. Statistical values of refractive errors of the subject sample. All values in diopters

	Right Eye			Left Eye		
	M (D)	J0	J45	M	J0	J45
Mean	-2.88	+0.064	-0.028	-2.94	+0.044	+0.027
StDev	2.48	0.135	0.090	2.66	0.113	0.086



Figures 3.1(a) and (b), for right and left eyes, respectively show the distributions of spherical equivalent (M). Figures 3.1(c) and (d) show the distribution of astigmatism, plotted as J_0 vs J_{45} . With-the-rule astigmatism is indicated in these figures as the positive mean J_0 value. Mirror image symmetry is indicated by approximately equal magnitudes of the three refractive components, and by the sign of oblique astigmatism, J_{45} . The opposite sign of J_{45} astigmatism indicates mirror symmetry between the left and right eyes.

A. Subjective Refraction Repeatability

The constancy, or repeatability, of this alternative refraction method was evaluated by analysis of test-retest differences. Refractions on both eyes were repeated within sessions and between sessions, and both types of test-retest differences are examined. Refractive powers are primarily expressed as spherical equivalent, or M , and the two components of astigmatism, J_0 and J_{45} . This expression of refractive powers, rather than sphere, cylinder and axis, is the appropriate form, as they are mathematically orthogonal, as described by Thibos *et al*, and others²⁹.

Table 3. Distributions (SDs) for Between- and Within-session Test-Retest differences.

	M (D)	J_0 (D)	J_{45} (D)
Between TRT	0.433	0.182	0.140
Within TRT	0.253	0.167	0.133

1. Between-Session Repeatability

Table 3 lists repeatability values for refractive parameters in the form of the standard deviation of test-retest differences. Figure 3.2 illustrates these distributions as histograms for the Between-session data. Each histogram represents the difference in dioptric power between the test and retest sessions. Means are close to zero, and none are significantly different from zero (all p-values > 0.4), indicating there was no systematic difference in the means between test and re-test. The table and figure show results for the right eye; left eye results are similar.

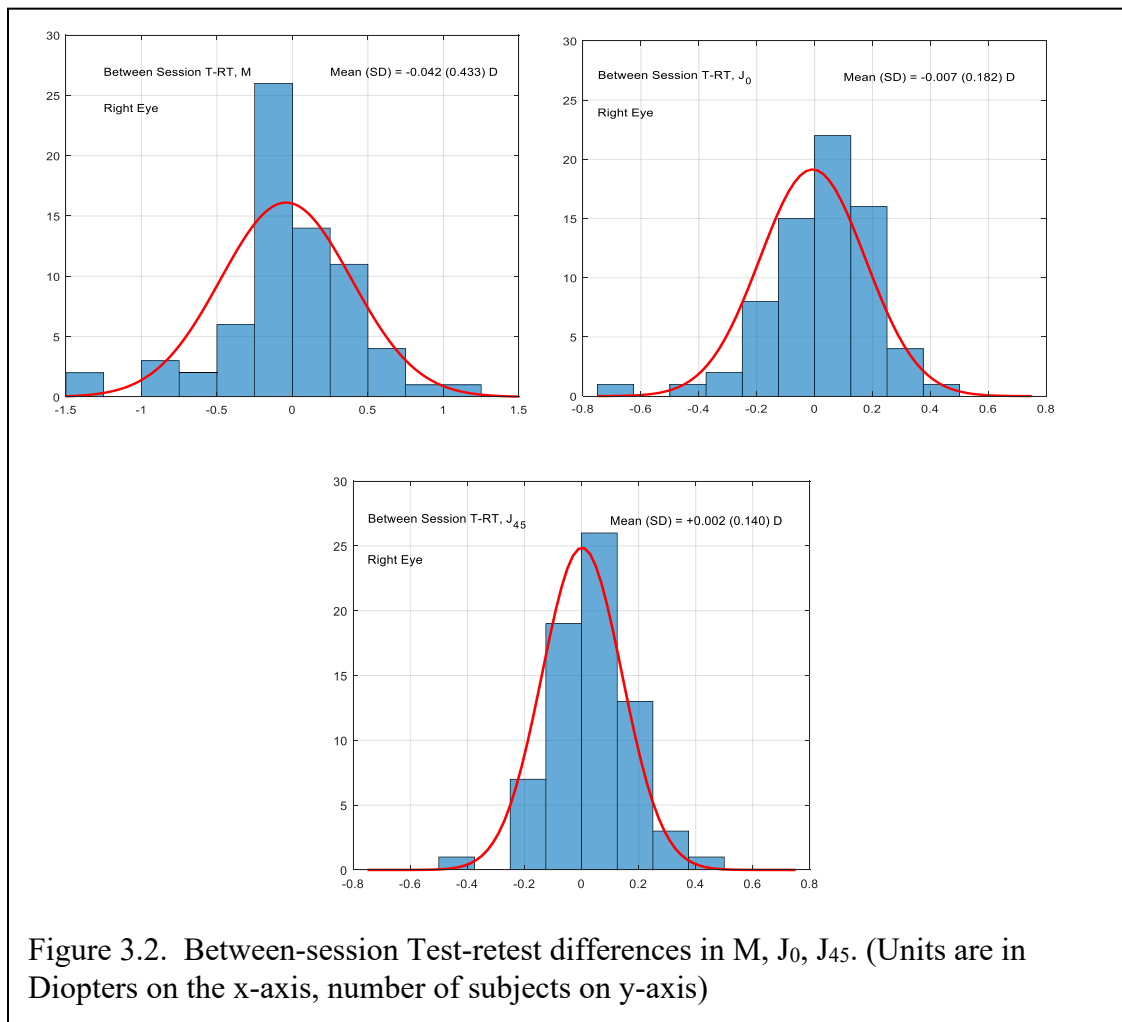
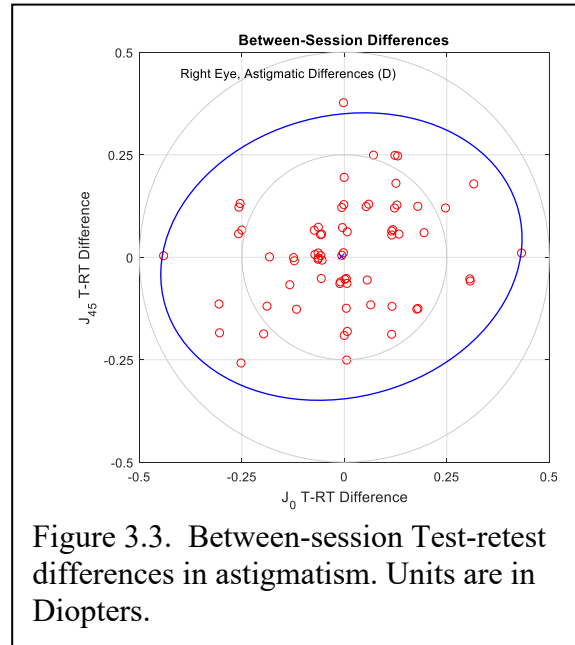


Figure 3.3 is based on the same between-session astigmatism data but plotted in a different format to illustrate a different aspect of the data. It plots J_0 and J_{45} on X and Y axes, showing their distribution across this plane. This type of (X, Y) plot is also known as the “plane of astigmatism”, or a “double angle” plot. This “double angle” term

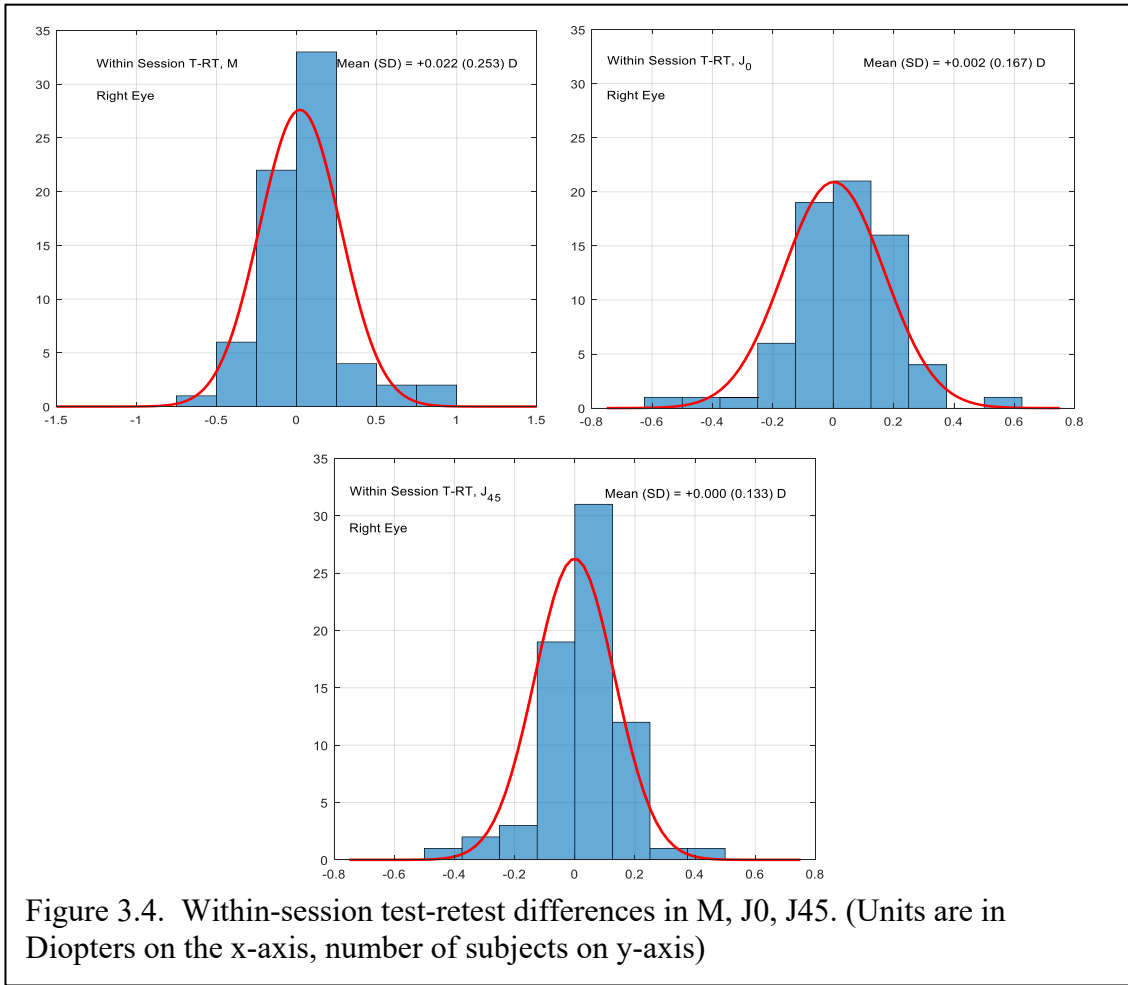


comes from the property that the orientation of the vector (i.e. the orientation of the line from the origin to the (x,y) position), is double the minus-cylinder axis. The 95% confidence ellipse is shown, meaning that 95% of the observations are expected to fall within this ellipse. This ellipse is generated from the covariance matrix of J_0 and J_{45} . The values in Table 3.2, and this ellipse, shows that the variability in J_0 is slightly larger than that of J_{45} .

1. Within-Session Repeatability

Table 3 also includes values for within-session test-retest difference distributions.

Figures 3.4, and 3.5 illustrate these within-session test-retest differences as histograms, and on a double-angle plot. These within-session distributions are slightly narrower than the corresponding between-session



distributions. Figure 3.5 illustrates the test-retest difference in the astigmatic components. It shows J₀ and J₄₅ plotted on the plane of astigmatism, with most data points falling within 0.25 D of the (0,0) point.

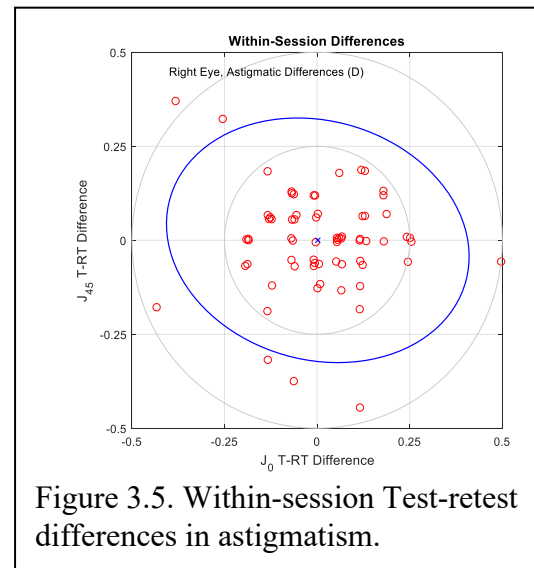
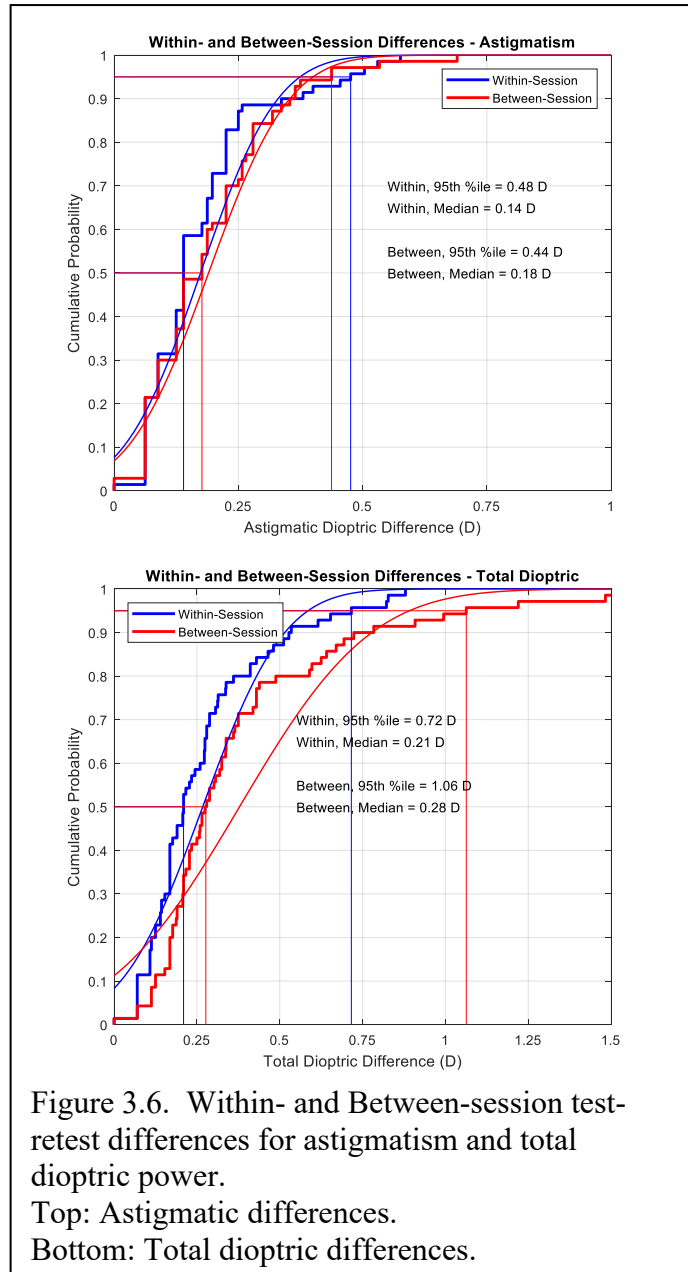


Figure 3.6 consists of cumulative probability plots for astigmatic and total dioptric powers, comparing within- and between-session test-retest differences. The step-wise curves are the empirical cumulative probabilities. The smooth curves are the best-fitting cumulative normal probabilities. Each curve represents the probability that a given data point falls at or below a certain dioptric value. The plots allow a more direct comparison of these repeatability values. The top panel shows astigmatic differences, and the cumulative normal curves fit the empirical



data reasonably well. It is seen that there is little difference between the test-retest values, regardless of whether the tests were performed minutes, or days, apart. In fact, the 95th percentile value for the empirical within-session difference is slightly larger than the between-session difference.

The lower panel shows the total dioptric differences for the two test-retest measures. For total dioptric difference, the cumulative normal curves fit the empirical data less well. Test-retest differences within a session are smaller than test-retest differences between sessions. Total dioptric power incorporates spherical power differences. Astigmatic differences alone were not substantially different within and between sessions.

B. Comparison to Standard Subjective Refraction

As described in the Methods section, the repeatability of this meridional refraction method is compared to that of standard subjective refraction. The repeatability of standard subjective refraction is taken from studies of normal subjects, in which refraction was performed under a prescribed protocol at two sessions^{13, 30, 37} The results reported here are discussed in the context of those studies in the Discussion section.

C. Subjective Refraction – Validity:

Validity, or accuracy, in this context, is based on the assertion that a refractive correction that enables better visual acuity is more accurate. Visual acuity was measured with each refractive result, using a method designed to yield a more precise estimate of

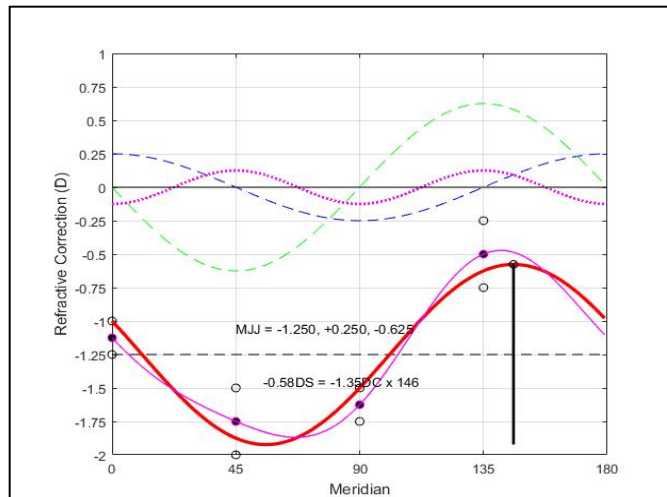


Figure 3.7. Datapoints at the four cardinal meridians used to generate the Measurement SD. In this case, for those four meridians, ($p_{i,1}$ and $p_{i,2}$) are (-1, -1.25), (-1.5, -2), (-1.5, -1.75), and (-.25, -.75). These particular data yield an MSD of 0.1563 D.

acuity via computer assisted adaptive VA measurements.

The data from this study were generated from a single refraction technique, so it is not possible to directly compare the accuracy of this technique to another. It is possible, however, to explore the relationship between quality of fit of the data to the visual acuity achieved with each refraction. One reasonable expectation is that the more variable the data or subjective findings during refraction, the poorer the visual acuity to be expected. For example, a particular subject may be very inconsistent in their responses for each meridian tested. The result of that refraction could be expected to be less accurate, resulting in poorer acuity.

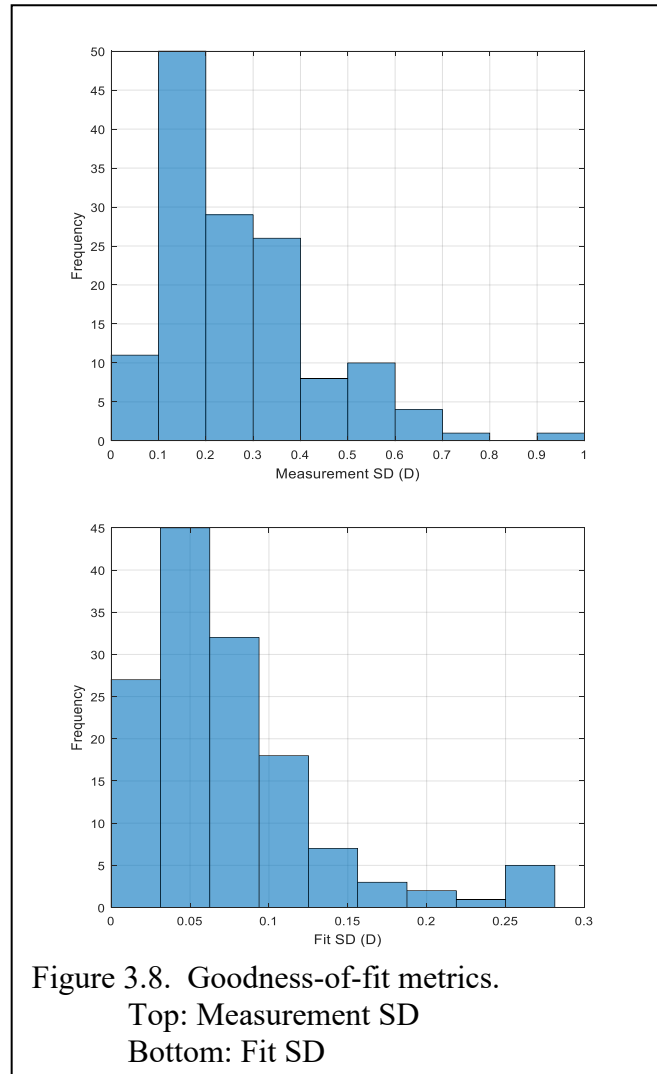
There are two metrics of the quality of the fit in the empirical data: metric (1) is generated from the differences in the dioptric endpoints at each orientation, and (2) is generated from how closely the fitted one-cycle sinusoid fits the empirical data. Figure 3.7 illustrates these metrics. Metric (1), called “Measurement SD”, or MSD, is derived from the two measured powers at each orientation. The MSD equals the square root of the mean of the squared differences at each orientation, or more formally (as described in

Methods): $MSD = \sqrt{\frac{\sum_{i=1}^4 (p_{i,2} - p_{i,1})^2}{4}}.$

The second fit metric, called fit standard deviation represents the mis-match between the mean value of the data at each orientation and the value of the best-fitting one-cycle sinusoid at that orientation. In Fig. 3.7, those points are: -1.125, -1.875, -1.5, and -1.625 D. When that one-cycle sinusoid is found via a discrete Fourier transform, the fit standard deviation is equal to the amplitude of the two-cycle sinusoid that is part of the

output from the discrete Fourier transform. In Fig 3.7, that is the dotted, magenta 2-cycle sinusoid, which in this case has an amplitude of 0.125 D. The 2-cycle sinusoid is the difference in fit between each meridian endpoint and the spherocylindrical correction at that meridian. Note that at each of the four orientations, the bold red curve (i.e. the refractive correction) misses the mean of the data by 0.125 D.

Figure 3.8 shows the distributions of these two metrics



for the right eyes of the subjects. It was expected that each of these metrics would be related to the visual acuity achieved with each refraction. Figure 3.9 shows the relationship between Measurement SD to logMAR visual acuity, and Fit SD to logMAR visual acuity. Both figures show that as each metric increases, visual acuity worsens; however, there is only a statistically significant relationship for the MSD metric.

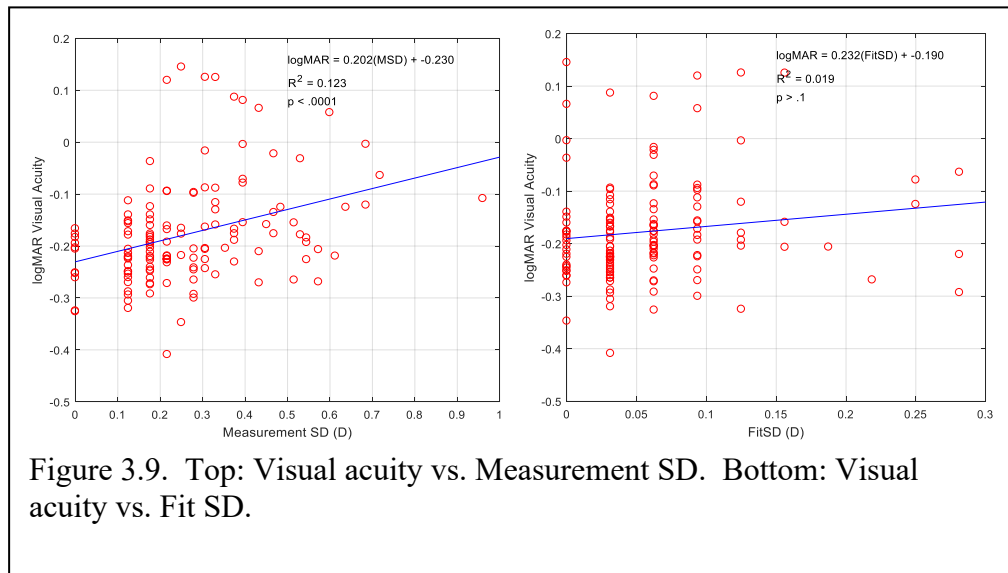


Figure 3.9. Top: Visual acuity vs. Measurement SD. Bottom: Visual acuity vs. Fit SD.

D. Test Duration

The overall duration of each test session was timed, beginning with the start of the first refraction to the end of the last visual acuity measurement. This distribution is shown in Figure 3.10. The mean duration is 48.7 minutes (SD = 11.5 minutes). Each session included four refractions (i.e. 2 refractions x 2 eyes), and a visual acuity measurement with the result of

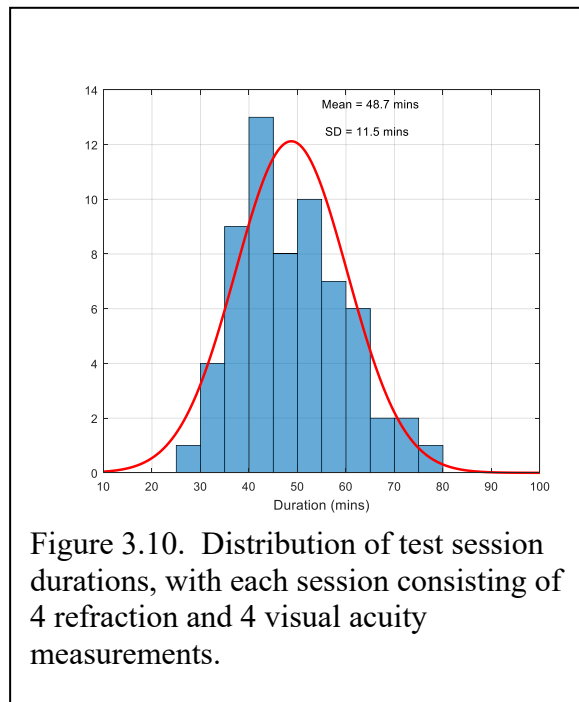


Figure 3.10. Distribution of test session durations, with each session consisting of 4 refraction and 4 visual acuity measurements.

each refraction. This results in approximately 12 minutes per eye for refraction and acuity testing. The acuity measurement was more prolonged than what would be found

in a typical clinical setting, since it employed the adaptive staircase procedure described in the Methods section. It is estimated that the duration of a refraction plus VA measurement was about 40% refraction and 60% acuity measurement. That proportion results in each refraction taking, on average, 40% of 12 minutes, or 4.8 minutes.

Chapter 4: Discussion

Many factors currently limit access to receiving correction of refractive error, most of which stem from the socioeconomic status of an individual or community. The goal of this study was to establish an alternative subjective refraction technique that would effectively address these barriers. While limitations vary based on location, the focus was not to replace the current gold standard subjective refraction technique where access isn't limited due to availability. A person's financial situation acts as a large barrier to many people in the United States; however, programs to provide needed eye care including refraction to people in need are better suited as a solution than this proposed alternative. In many countries the measurement and correction of refractive error is limited or even unavailable due to the cost of equipment and requirement of trained clinicians. This refraction technique was originally developed to address these factors.

In this study, a Greens Refractor was used to present spherical lenses to the subject. The use of a phoropter allows for spherical and cylindrical lenses to be quickly shown to a patient, including a Jackson cross cylinder lens (JCC) that is used to refine cylindrical power and orientation. This piece of equipment is an example of an expensive barrier to refraction. Trial frame refraction is a less expensive tool that can replace the need for a phoropter; however, a trial frame and lens set are still marginally expensive

and require an experienced clinician to use correctly. The need for expensive equipment, and more complicated lens presentations is due primarily to cylinder correction.

Cylindrical lenses are required for most refractions to correct for the presence of astigmatism. For this vector refraction, linearly oriented targets were used to isolate each of the four cardinal meridians so that spherical lenses alone were needed. For each meridian a blurred to unblurred spherical power check was used as in the beginning of typical standard refraction. Because each meridian was separately refracted, there is no need for cylindrical lenses or JCC lenses. The alternative technique in this study utilized only the first step of typical subjective refraction, spherical lens check, which consists of blurred to not blurred presentation of increasing minus powered lenses until contrast was maximized. This simple increase and decrease in spherical lens power could be performed by a novice clinician with limited training. To test this aspect, this study was performed by an optometry student between their first and second year of study. Students at this point in the curriculum have limited clinical experience and no experience with performing refraction. They had been introduced to optical correction of refractive error, however they had yet to be taught clinical refraction, and had no experience in clinic refracting patients. The procedure tested in this study would allow for easier training for someone to perform this test, and thus increase availability of available clinicians.

It is appropriate to assume that this technique could be performed with other methods of presenting spherical lenses other than with a phoropter. A phoropter is an example of an expensive piece of equipment that requires trained personnel to operate. The use of a retinoscopy lens bar set allows for multiple different lenses to be presented

as with a phoropter. While most retinoscopy lens bar sets come in half or full diopter steps, ancillary quarter lenses could be utilized to refine refractions. The cost of retinoscopy bar sets ranges from 40-70 dollars. In comparison a used phoropter can cost between two and four thousand dollars without a stand mount. With increased access to refraction there should be an additional increase in access to correction. There are many programs that donate previously used glasses or inexpensive materials such as a Lion's Club, New Eyes, and SVOSH at optometry schools.

It is essential that a clinical test have the ability to produce consistent results. In this study, repeatability was evaluated by a test-retest statistic of both within and between session refractions. The mean test-retest values found in this study were not statistically different from zero, indicating no bias between the test and retest. While this shows the proposed alternative technique produces repeatable test results, it must be compared to current standard of care. Accepted test-retest data of previous studies on subjective refraction are shown in Table 4. The values represent standard deviation of test-retest distributions from non-cycloplegic subjective refraction studies, in which test and retest were performed at least one day apart. The data from the current study used a subjective criterion of maximum plus for highest contrast and/or sharpest edges in separate meridians. The other listed studies are of standard subjective refraction using the Jackson cross-cylinder for astigmatic determination and a subjective criterion of maximum plus for highest contrast and/or best visual acuity.

Table 4. Between-session test-retest repeatability of subjective refraction. All values are the standard deviation of the distribution of test-retest differences in the three refractive components. See references for specifics of individual studies.

	M (D)	J₀ (D)	J₄₅ (D)
Lehman (2020)	0.433	0.182	0.140
Pesudovs ³⁸ (2007)	0.245	0.102	0.066
Raasch ³⁰ (2001)	0.260	0.117	0.082
Bullimore ¹³ (1998)	0.395	0.194	0.165
Elliott ³⁷ (1997)	0.283	0.132	0.125

Table 4 shows that refraction in the current study is generally less repeatable than in standard subjective refraction (1.46x, 1.34x, and 1.28x the mean values for M, J₀, and J₄₅, respectively). There are several explanations to the comparative lack of consistency. Standard subjective refraction is a highly refined clinical procedure that has withstood the test of time; it is often considered the “gold standard” for refraction, at least for young, normal patients similar to the subject sample in this study. The goal of this study was not to improve upon or replace this gold standard. Rather, the purpose was to evaluate an alternative technique, to determine whether it performs comparably to standard refraction, while meeting situational restrictions to increase access.

Variability of the spherical equivalent M, was greater than the two astigmatic components J₀ and J₄₅, as seen in Table 4. While the overall spherical component had increased test-retest, each meridian had equal test-retest repeatability indicating consistency of refraction across all meridians. If J₀ and J₄₅ were more variable, this would indicate that there was inconsistency between meridians, questioning the accuracy of the refraction. From the between- and within-session repeatability values, speculative

inferences can be made about how much actual change in refractive error occurred between sessions. If it is assumed that changes in M, J0, and J45 occur independently, then the variances add. That is, the variance of the between-session test-retest difference equals the variance of the within-session test-retest difference plus the variance of the actual change in refractive power of the eye. Specifically, for M, that would be:

$\sigma_B^2 = \sigma_W^2 + \sigma_C^2$, where σ^2 represents variance, and the subscripts B, W, and C represent Between-session, Within-session, and actual Change, respectively. For M, the numbers yield:

$$0.433^2 = 0.253^2 + C^2 \quad C^2 = 0.1235 \quad C = 0.35,$$

where C is a standard deviation and gives some indication of how much change actually occurred between sessions. Similar analyses for the astigmatic components yield values of 0.072 D for J₀, and 0.044 D for J₄₅. These numbers certainly should be interpreted with caution, as it is unlikely that the change in the three refractive components change independently between sessions. If they are not independent, then simply adding the variances without considering covariances is not fully accurate. However, the numbers may give some relative indication of which of the three components actually changes the most; in this case M. That observation lends support to the idea that changes between sessions are likely due to changes in the overall power of the eye, due perhaps to changes in accommodative level, or to varying levels of success in controlling over-minusing.

Current gold standard subjective refraction utilizes recognition acuity and other techniques to control for spherical equivalent variability. These same techniques could be employed alongside this alternative method. A patient's ability to accommodate increases

the refractive power of the eye. The accommodative system includes four “types” of accommodation, tonic, proximal, convergence, and reflexive. The accommodative state of an individual can fluctuate; and if not controlled for can cause variability. While this mechanism can be paralyzed with topical cycloplegic diagnostic drops, there are other methods to stabilize accommodation, and control excess minus power. Commonly at the end of refraction BCVA will help determine the spherical endpoint. It is well known that subjects will tend to accept more minus than needed during refraction. While acuity does not improve, the size of the object decreases giving the perception of increased contrast and clarity. To combat this, clinicians will only present up to -0.75D past when the patient can first read the 20/20 line. Another strategy to avoid giving excess minus power is to use the duochrome test. The duochrome test relies on chromatic aberration; colors of shorter wavelength are refracted more, or in front of, colors of longer wavelength. As a result, an eye is effectively more myopic for green than it is for red. In the duochrome test, a chart with a background that is red on one side and green on the other is shown to the patient. The optimum spherical power end point is identified by the sphere power that either equalizes the clarity of the letters on red and green, or with a slight bias toward the red, i.e. toward the more hyperopic correction.

In Table 4, the values shown are from studies performed by experienced clinicians. As previously mentioned, in this study refractions were performed by a relatively novice clinician, with little previous experience. Without experience interpreting subjective responses determining a correct endpoint is more difficult. While

the aspect of cylindrical refraction was removed, there is still inherent difficulty administering subjective tasks.

Additionally, there was no additional testing or checks to avoid over-minusing or to control for accommodation. During standard refraction, change in acuity is used in addition to subjective response of the patient. Letters, numbers, or oriented figures such as Landolt rings can be used in a check of over-minusing: the clinician can check to see if visual acuity improves, or not, when the subject states that the image is clearer. In the current study, no similar opportunity to check was available.

One significantly important factor in subjective refraction is balancing the prescription in both eyes. This ensures that stimulus to accommodate is equal between the two eyes, important for preventing eye strain, ensuring clear comfortable vision between both eyes, and promoting stability for the accommodative system. Common tests to balance a patient's final prescription were not used in this study but are commonly used in tandem with standard subjective refraction, such as dissociated blurred balance, or the use of polarized lenses or dissociated duochrome test.

Variability of within-session test-retest is better, or less, than between-session test-retest. It is more likely that an actual change would have occurred from one visit to the next, compared to a real change within a visit. The ratio of mean test-retest comparing between- and within-session refractions also indicate that change occurs in M rather than J0 or J45. This may be because, between the two test dates, there might be an actual change, and it would be seen as a change in the M, not the J0 or J45 components.

For both Between- and Within-session test-retest, the astigmatic components J_0 and J_{45} were more repeatable than the spherical equivalent M. If tested with gold standard subjective refraction that included methods to better control over-minusing, it is expected that the repeatability of the spherical equivalent would be better in this alternative method. However, the repeatability of the astigmatic components would likely be very similar. If methods were incorporated into this meridional method to better control over-minusing, we would expect to see better test-retest repeatability in this study. The improvement would most likely be primarily in the M component of refractive power. Within-session repeatability is somewhat better than between-session repeatability, as shown in Table 5.

Table 5. Between- and Within-session repeatability.			
	Between	Within	Ratio
M	0.433	0.253	0.58x
J_0	0.182	0.167	0.92x
J_{45}	0.140	0.133	0.95x

One important consideration in any clinical test is the length of test time needed to arrive at an endpoint. A longer test may fatigue or lose the attention of a subject, resulting in data that can be misleading or incorrect. The amount of time for subjective refraction depends on the number of lens presentations shown to a subject, and the amount of time a subject needs to respond. Some individuals require multiple presentations for each step (the classic case of the engineer as a patient), while others may make judgments much more quickly. Comparing the number of lens presentations for both the alternative

technique and standard refraction, it is expected that test durations would be similar. Four meridians were refracted twice, with an estimated 5-6 lens presentations at each (and “which is better one or two?” questions and answers), resulting in between 40-48 iterations. In a standard subjective refraction, there is typically a spherical check, a cylinder power check, a cylinder axis check, a cylinder power re-check, and a spherical re-check, resulting in a total number of lens comparisons ranging from 30-40. In addition, it could be that subjective comparisons of cylindrical lens changes in power and axis may be more difficult judgments than spherical changes, and therefore could require more time.

The total time of each visit was timed using a Matlab internal timer for running the program. The average estimated time for a refraction in this study took 4.8 minutes. This included two refractions in each of the four respective meridians. This is very comparable to published average times for subjective refraction. There have been few studies done on the timing of subjective refraction. The existing published data does suggest mean times for subjective refraction range between 4:15 to 5:36 with a standard deviation of 1-2 minutes³⁹. These times were the average from three experienced optometrists on 99 subjects.

No objective refraction methods such as retinoscopy or a preliminary auto-refractor measurement were used to provide a starting point for subjective refraction in this study. Large lens power changes were made in the first few lens trials to ensure that that meridian was over-plussed before making smaller changes in lens power during each meridian’s refraction. That could have resulted in longer refraction times than if a more

precise starting point had been established. After the first refraction a general starting point was established for the second refraction of the session.

Another aspect in this study was that the subjects were asked to judge the clarity/blur of an unfamiliar target. A potential benefit of using letters is that patients may be able to make judgments of clarity more easily when viewing a familiar target such as a letter. With this technique, it may have taken some time for the subject to become comfortable with making judgments of this type of target. The target was demonstrated to the subject at the first visit with their current correction. For individuals without a previous correction, a description of the line targets would have to be given in more detail.

An adaptive, maximum-likelihood visual acuity technique was used in this study. Each measurement consisted of 50 letter presentations using a strategy that was designed to concentrate most letter presentations near the current estimate of threshold letter size. A learning or fatigue effect was not observed with this more prolonged test procedure, but that possibility cannot be excluded. It is possible the prolonged acuity test could have affected the acuity measurement, or the refraction, due to inattention or fatigue. During the VA test, the subject is presented with a ten-alternative forced choice. The refraction method is a modified two-alternative forced choice test, perhaps requiring less cognitive load than the acuity test. Because the subject may be less engaged in choosing a response during refraction, the final endpoint could have been affected.

This computer-assisted adaptive visual acuity measurement was previously compared to a standard ETDRS visual acuity measurement in a previous MS thesis

project. Using those data, the method was refined and tested through computer simulation. Those simulations are based upon a “virtual” subject represented by a probability of seeing (POS) function. That function has two parameters: position and slope. It relates the size of a given optotype to the probability, from 0.0 to 1.0, of a correct response (corrected for a 10% chance of a correct guess). The letter size at which the function crosses the 50% correct level defines the threshold letter size. The slope represents the rate of transition from a probability of a correct response approaching 0% at small letter sizes to a probability that approaches 100% correct at larger letter sizes. A steep slope represents a sharper transition between incorrect and correct letter identification, and results in better repeatability. Part of the refinements in the procedure involved more accurate estimates of the steepness parameter, which produces more realistic simulations. Those simulations enabled selection of adaptive test variables that improve the repeatability of the results. The adaptive method also provides greater resolution in letter sizes than a standard ETDRS test. For example, an individual may correctly identify every letter on the 20/25 line, but none on the 20/20 line. The true threshold could be anywhere between those two acuity levels. The adaptive procedure would be more capable of accurately finding that threshold level.

A clinical test must be repeatable and accurate in order to provide clinically useful or meaningful data. While this study did not compare the proposed alternative method to current subjective refraction, previously published data can be used. Two metrics were used to determine and evaluate accuracy. The first evaluated the difference between the two measurements taken at each respective meridian. Theoretically, if a subject's

responses within refraction are more consistent, the endpoint will be more accurate and should yield a better VA. This metric termed measurement standard deviation (MSD) had a statistically significant positive correlation with final visual acuity.

The second metric of accuracy examined the difference between the resultant spherocylindrical one-cycle sinusoid and the determined refractive error of each respective meridian, termed fit standard deviation. While there was correlation between better fit (smaller fit standard deviation) and visual acuity, the relationship was not statistically significant. However, if the tested population included more subjects with significant higher order aberrations, the fit standard deviation could potentially play a more important role. One difficulty of refraction of patients with visually significant higher order aberrations influencing refractive error, is that standard subjective refraction is increasingly difficult. Using repeated 2-alternative forced tests, end points occur when there is no noticeable difference between options. When an endpoint is bracketed it is assumed that there is now no change in lenses that could improve acuity. However, with highly aberrated eyes, best clarity is harder to subjectively discern. For example, the optotype letter E for a person with only spherical refractive error, when fully corrected both horizontal and vertical lines, is clear. For a patient with with-the-rule astigmatism, the horizontal and vertical lines require different powers to be equally clear. For a patient with higher order aberrations, clarity may fluctuate across the letter without a symmetric or even pattern. Thus, discerning which is better produces larger and more inaccurate endpoints. Within this study, linear optotype targets help simplify this problem.

While it was not the original intent of the study, this new refraction protocol could also be utilized for patients with higher order aberrations. There are multiple causes of visually significant higher order aberrations causing decreased vision due to limits in correction. One of the most studied causes for higher order aberrations is keratoconus, a corneal ectasia, non-inflammatory bilateral asymmetric progressive thinning of the cornea. Depending on the progression of the condition, keratoconus can be corrected with spectacles, or contact lenses of different kinds. Spherocylindrical lenses do not correct the higher order aberrations such as coma, spherical aberration, or trefoil. While RGP and scleral lenses can create a smoother surface interaction due to the interaction of the lens cornea and tear film, there are still limits to correction. During refraction, higher order aberrations create difficulty for patients to discern clarity with complex optotypes with multiple orientations of lines. For this reason, refraction of isolated meridians using spherical lenses and linear targets could potentially allow for easier subjective refraction in these cases. Fit standard deviation, the goodness of fit metric that analyzes how the one-cycle sinusoid spherocylindrical lens power differs from each meridian did not have statistically significant correlation with visual acuity. However, if tested on eyes with high levels of aberration, the expectation is that this goodness-of-fit metric would become significant.

The subjects used in this study aligned with the expected distribution of refractive error with a majority having low to moderate myopia, and a low amount of with-the-rule astigmatism.³⁰ It was expected that visual acuity would correlate with the fit of the one-cycle sinusoid; however, it is not surprising that this was not statistically significant. In

clinical practice, patients with normal refractive error and low amounts of higher order aberration, have a range of correction that produces acceptable and clear vision.

This study examined subjective refraction but raises the question of whether an objective version of meridional refraction could be developed. That type of objective method could consist of using aberrometry data to calculate the lens powers that produce maximum grating contrast at multiple orientations. This would essentially be using a computer, rather than the subject, to decide what lens power is best at each orientation. That question is beyond the scope of this study but suggests future work.

Currently this technique is being further studied to determine its application to those with HOAs. The use of wavefront aberration measurements to determine the needed spherocylindrical lens is being compared to standard subjective refraction and this subjective technique. The application of this technique on highly aberrated eyes may be promising and could potentially serve a purpose for patients who are difficult to refract due to high levels of aberration. The effect of cycloplegia, to address the issue of overminusing is also a future research direction.

This study has shown that repeatability of this refraction technique is comparable to the current gold standard subjective refraction. It was also shown that the equipment and personnel required for performing this process would potentially increase availability of refraction, helping solve a world issue of uncorrected refractive error. There are additions that need to be made to better control accommodation and prevent overminusing. There are also potential applications of this refraction that could be utilized for those with higher order aberrations.

Bibliography

1. Benjamin WJ, Borish IM. Borish's clinical refraction. 2nd ed. St. Louis Mo.: Butterworth Heinemann/Elsevier; 2006.
2. Mutti DO, Mitchell GL, Jones LA, Friedman NE, Frane SL, Lin WK, et al. Axial growth and changes in lenticular and corneal power during emmetropization in infants. *Invest Ophthalmol Vis Sci*. 2005; 46:3074-80.
3. Jones-Jordan LA, Sinnott LT, Cotter SA, Kleinstein RN, Manny RE, Mutti DO, et al. Time outdoors, visual activity, and myopia progression in juvenile-onset myopes. *Invest Ophthalmol Vis Sci*. 2012; 53:7169-75.
4. Holden BA, Fricke TR, Wilson DA, Jong M, Naidoo KS, Sankaridurg P, et al. Global Prevalence of Myopia and High Myopia and Temporal Trends from 2000 through 2050. *Ophthalmology*. 2016; 123:1036-42.
5. Zadnik K, Sinnott LT, Cotter SA, Jones-Jordan LA, Kleinstein RN, Manny RE, et al. Prediction of Juvenile-Onset Myopia. *JAMA Ophthalmol*. 2015; 133:683-9.
6. Walline JJ, Robboy MW, Hilmantel G, Tarver ME, Afshari NA, Dhaliwal DK, et al. Food and Drug Administration, American Academy of Ophthalmology, American Academy of Optometry, American Association for Pediatric Ophthalmology and Strabismus, American Optometric Association, American Society of Cataract and Refractive Surgery, and Contact Lens Association of Ophthalmologists Co-Sponsored Workshop: Controlling the Progression of Myopia: Contact Lenses and Future Medical Devices. *Eye Contact Lens*. 2018; 44:205-11.
7. Fang PC, Chung MY, Yu HJ, Wu PC. Prevention of myopia onset with 0.025% atropine in premyopic children. *J Ocul Pharmacol Ther*. 2010; 26:341-5.
8. Wu PC, Tsai CL, Wu HL, Yang YH, Kuo HK. Outdoor activity during class recess reduces myopia onset and progression in school children. *Ophthalmology*. 2013; 120:1080-5.
9. Paune J, Morales H, Armengol J, Quevedo L, Faria-Ribeiro M, Gonzalez-Mejome JM. Myopia Control with a Novel Peripheral Gradient Soft Lens and Orthokeratology: A 2-Year Clinical Trial. *Biomed Res Int*. 2015; 2015:507572.
10. Cotter SA. Management of childhood hyperopia: a pediatric optometrist's perspective. *Optom Vis Sci*. 2007; 84:103-9.
11. Maria Revert A, Conversa MA, Albarran Diego C, Mico V. An alternative clinical routine for subjective refraction based on power vectors with trial frames. *Ophthalmic Physiol Opt*. 2017; 37:24-32.
12. Khurana AK. Theory and Practice of Optics and Refraction: Elsevier; 2008.

13. Bullimore MA, Fusaro RE, Adams CW. The repeatability of automated and clinician refraction. *Optom Vis Sci.* 1998; 75:617-22.
14. Otero C, Aldaba M, Pujol J. Clinical evaluation of an automated subjective refraction method implemented in a computer-controlled motorized phoropter. *J Optom.* 2019; 12:74-83.
15. Tahhan N, Fricke TR, Naduvilath T, Kierath J, Ho SM, Schlenther G, et al. Uncorrected refractive error in the northern and eastern provinces of Sri Lanka. *Clin Exp Optom.* 2009; 92:119-25.
16. Lou L, Yao C, Jin Y, Perez V, Ye J. Global Patterns in Health Burden of Uncorrected Refractive Error. *Invest Ophthalmol Vis Sci.* 2016; 57:6271-7.
17. Tahhan N, Papas E, Fricke TR, Frick KD, Holden BA. Utility and uncorrected refractive error. *Ophthalmology.* 2013; 120:1736-44.
18. Pizzarello L, Abiose A, Ffytche T, Duerksen R, Thulasiraj R, Taylor H, et al. VISION 2020: The Right to Sight: a global initiative to eliminate avoidable blindness. *Arch Ophthalmol.* 2004; 122:615-20.
19. Raasch TW. Spherocylindrical refractive errors and visual acuity. *Optom Vis Sci.* 1995; 72:272-5.
20. DALYs GBD, Collaborators H, Murray CJ, Barber RM, Foreman KJ, Abbasoglu Ozgoren A, et al. Global, regional, and national disability-adjusted life years (DALYs) for 306 diseases and injuries and healthy life expectancy (HALE) for 188 countries, 1990-2013: quantifying the epidemiological transition. *Lancet.* 2015; 386:2145-91.
21. Chadha RK, Subramanian A. The effect of visual impairment on quality of life of children aged 3-16 years. *Br J Ophthalmol.* 2011; 95:642-5.
22. Wolffsohn JS, Cochrane AL. Design of the low vision quality-of-life questionnaire (LVQOL) and measuring the outcome of low-vision rehabilitation. *Am J Ophthalmol.* 2000; 130:793-802.
23. Smith TS, Frick KD, Holden BA, Fricke TR, Naidoo KS. Potential lost productivity resulting from the global burden of uncorrected refractive error. *Bull World Health Organ.* 2009; 87:431-7.
24. Fricke TR, Holden BA, Wilson DA, Schlenther G, Naidoo KS, Resnikoff S, et al. Global cost of correcting vision impairment from uncorrected refractive error. *Bull World Health Organ.* 2012; 90:728-38.
25. Raasch T. Clinical refraction in three-dimensional dioptric space revisited. *Optom Vis Sci.* 1997; 74:376-80.
26. Flaxman SR, Bourne RRA, Resnikoff S, Ackland P, Braithwaite T, Cicinelli MV, et al. Global causes of blindness and distance vision impairment 1990-2020: a systematic review and meta-analysis. *Lancet Glob Health.* 2017; 5:e1221-e34.
27. Resnikoff S, Pascolini D, Etya'ale D, Kocur I, Pararajasegaram R, Pokharel GP, et al. Global data on visual impairment in the year 2002. *Bull World Health Organ.* 2004; 82:844-51.
28. Johnson GJ. Vision 2020: The Right to Sight: Report on the Sixth General Assembly of the International Agency for the Prevention of Blindness (IAPB). *Community Eye Health.* 1999; 12:59-60.

29. Thibos LN, Wheeler W, Horner D. Power vectors: an application of Fourier analysis to the description and statistical analysis of refractive error. *Optom Vis Sci.* 1997; 74:367-75.
30. Raasch TW, Schechtman KB, Davis LJ, Zadnik K, Study CSGCLEoK. Repeatability of subjective refraction in myopic and keratoconic subjects: results of vector analysis. *Ophthalmic Physiol Opt.* 2001; 21:376-83.
31. Andrews EJ. Computer-assisted Adaptive Methods of Measuring Visual Acuity. Columbus OH: Ohio State University; 2017.
32. King-Smith PE, Grigsby SS, Vingrys AJ, Benes SC, Supowit A. Efficient and unbiased modifications of the QUEST threshold method: Theory, simulations, experimental evaluation and practical implementation. *Vision Research.* 1994; 34:885-912.
33. Pentland A. Maximum likelihood estimation: The best PEST. *Perception & Psychophysics.* 1980; 28:377-9.
34. Gekeler F, Schaeffel F, Howland HC, Wattam-Bell J. Measurement of astigmatism by automated infrared photorefractometry. *Optometry and vision science : official publication of the American Academy of Optometry.* 1997; 74:472-82.
35. Raasch TW. Corneal topography and irregular astigmatism. *Optometry and vision science : official publication of the American Academy of Optometry.* 1995; 72:809-15.
36. Harris WF. Power vectors versus power matrices, and the mathematical nature of dioptric power. *Optometry Vision Sci.* 2007; 84:1060-4.
37. Elliott M, Simpson T, Richter D, Fonn D. Repeatability and accuracy of automated refraction: a comparison of the Nikon NRK-8000, the Nidek AR-1000, and subjective refraction. *Optom Vis Sci.* 1997; 74:434-8.
38. Pesudovs K, Parker KE, Cheng H, Applegate RA. The precision of wavefront refraction compared to subjective refraction and autorefractometry. *Optometry Vision Sci.* 2007; 84:387-92.
39. Carracedo G, Carpena-Torres C, Serramito M, Batres-Valderas L, Gonzalez-Bergaz A. Comparison Between Aberrometry-Based Binocular Refraction and Subjective Refraction. *Transl Vis Sci Technol.* 2018; 7:11.